



National Center for Theoretical Sciences

THE MORBIDOSTAT: A BIO-REACTOR THAT PROMOTES SELECTION FOR DRUG RESISTANCE IN BACTERIA

ZHENZHEN CHEN

SZE-BI HSU

YA-TANG YANG

NCTS/Math

Technical Report

2018-019

THE MORBIDOSTAT: A BIO-REACTOR THAT PROMOTES SELECTION FOR DRUG RESISTANCE IN BACTERIA*

ZHENZHEN CHEN[†], SZE-BI HSU[‡], AND YA-TANG YANG[§]

Abstract. A morbidostat is a bacteria culture device that maintains a nearly constant microbial population for the selection of drug-resistant mutants via a feedback algorithm. In this paper, the global dynamics of a microbial species undergoing sequential evolution are studied in detail to elucidate the operation of a morbidostat. The cultivation of the microbes is assumed to be under periodic dilution, and a simple threshold algorithm is used as feedback. We also prove the extinction and uniform persistence of all species with both forward and backward mutation in a sequential evolution scenario. Numerical simulations for the case of logistic growth and the Hill function for drug inhibition are also applied to verify our theoretical results. The theoretical framework elucidates the generic features of the operation of a morbidostat under drug-inhibitor-induced feedback and will provide a useful aid for the design of experiments.

Key words. morbidostat, serial transfer dilution, wild type, mutants, exclusion principle, coexistence

AMS subject classifications. 34C, 92B, 94D

DOI. 10.1137/16M105695X

1. Introduction. Antibiotic drug resistance is a global health problem [1]. Today, clinically important bacteria are characterized by their resistance to single or multiple drugs. Antibiotic drug resistance mechanisms include (1) modification and deactivation of the antibiotic by expression of certain enzymes; (2) development of an active efflux for the drug; and (3) alteration of the intracellular drug target such as the ribosome, metabolic enzymes, or proteins involved in DNA replications or cell wall synthesis. The acquisition of high-level antibiotic resistance has been discovered in vivo. Historically, penicillin-resistant *Staphylococcus aureus* was discovered soon after the introduction of penicillin in clinical environments [2]. In a more recent example, antibiotic drug resistance has been studied by running the whole genome sequencing of clinical isolates from patients suffering from endocarditis (*S. aureus* infection of the heart muscle) and undergoing antibiotic treatment [3]. Through the course of infection over a 3-month period, a total of 35 point mutations were accumulated, many associated with the acquisition of antibiotic resistance. Increasing minimum inhibitory concentrations are also observed. Although the in vivo evolution of drug resistance can be studied retrospectively, these experiments lack systematic control over the environmental conditions for drug resistance. Alternatively, adaptive laboratory evolution can be used to study the molecular evolution of a microbial species undergoing selection pressure from antibiotic drugs [4]. Recently, many antibiotic-resistant

*Received by the editors January 15, 2016; accepted for publication (in revised form) November 16, 2016; published electronically March 23, 2017.

<http://www.siam.org/journals/siap/77-2/M105695.html>

Funding: The work of the authors was supported by the Ministry of Science and Technology, Taiwan (MOST), 105-2221-E-007-130-MY3.

[†]Department of Mathematics, Swinburne University of Technology, Melbourne VIC 3122, Australia (zhenzhenchen1221@yahoo.com).

[‡]Department of Mathematics and National Center of Theoretical Science, National Tsing Hua University, Hsinchu, Taiwan, Republic of China (sbhsu@math.nthu.edu.tw).

[§]Department of Electrical Engineering, National Tsing Hua University, Hsinchu, Taiwan, Republic of China (ytyang@ee.nthu.edu.tw).

evolution experiments have attempted to elucidate the emergence of antibiotic drug resistance under well-controlled laboratory conditions. For example, Austin’s group demonstrated that the drug concentration gradient can lead to the rapid emergence of antibiotic drug resistance in microfluidic devices [5]. Hwa’s group later developed a compartment model [6] to explain this phenomenon, based on the earlier theoretical consideration of stochastic evolution in a source and sink scenario [7]. Advances in synthetic biology and microfluidic techniques culminated in Hwa’s work on an experimentally validated model connecting the innate growth stability under the influence of translation-inhibiting antibiotic chloramphenicol to detailed biophysical processes and biochemistry such as passive diffusion and drug and enzyme interaction [8]. In short, during the microbial growth stage, the microbe can develop antibiotic drug resistance by constitutively expressing chloramphenicol acetyltransferase (CAT), an enzyme that deactivates chloramphenicol. The feedback model consists of an influx of chloramphenicol, microbial growth, and the CAT concentration.

Recently, a more advanced chemostat [9] known as a morbidostat has been developed with the aim of imposing drug selection pressure to induce mutations in a more systematic fashion [10]. A morbidostat is a microbial selection device that continuously adjusts the antibiotic concentration to maintain a nearly constant population. In one incarnation, as illustrated by Figure 1, the microbial population can be monitored by recording the optical density. The addition of the drug is computer-controlled based on a prescribed feedback algorithm. Samples are frozen daily to serve as the “fossil record” of the evolution, and a small fraction is used to inoculate a fresh batch of the medium and restart another growth cycle. After the experiment has run its course, the daily frozen samples are thawed and the inhibitor concentrations are characterized. These samples are also analyzed with whole genome sequencing techniques to reveal the molecular mechanism for the drug resistance. In this work, we present a theory to not only reproduce the essential features of this mechanism but also yield sufficient insight to provide guidelines for the analysis of the experimental data. It is our hope that the theory will aid the design of new experiments by identifying key parameters based on existing experimental data in the literature. The remainder of this paper is organized as follows. In section 2, we specifically introduce two deterministic

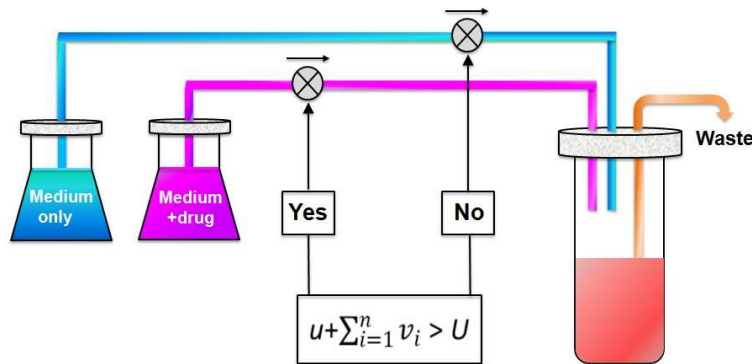


FIG. 1. A schematic of the morbidostat. A morbidostat is a continuous-culture device that automatically tunes inhibitor concentration to maintain constant growth inhibition. The assay runs in cycles of growth periods (T) and adds dilutions with either fresh medium (blue) or drug solution (magenta) based on a threshold feedback algorithm. The population is diluted with drug solution when the total bacteria density exceeds the preset threshold value (U).

models for the selection of drug-resistant bacteria in the morbidostat. The first one deals with sequential forward mutation with one wild type and N mutant species. The second model deals with the same sequential evolution but allows both forward and backward mutations. In section 3, we study the global dynamics of the morbidostat model in two cases and state the main results of this paper. The proofs are deferred to the appendix. In section 4, we present the results of numerical simulations with plausible parameters to verify key results on the global dynamics. Section 5 is the section of conclusion and discussion.

2. Description of our models. In the simplest scenario, we can formulate the transition from a wild type population to N mutant strains. In actual experiments conducted by Kishony's group [10], the device maintained a nearly constant population via computer-controlled feedback. The fitness test runs in cycles of growth periods T . For the forward mutation model (see Figure 2) and forward-backward mutation model (see Figure 3), the growth dynamics with the nutrient substrate S under the influence of the drug inhibitor P are given by models (2.1) and (2.2), respectively.

$$(2.1) \quad \begin{cases} \frac{dS}{dt} = -\frac{1}{\gamma}g_0(S)f_0(P)u - \frac{1}{\gamma}\sum_{i=1}^N g_i(S)f_i(P)v_i, \\ \frac{du}{dt} = g_0(S)f_0(P)u - q_0u, \\ \frac{dv_i}{dt} = g_i(S)f_i(P)v_i + q_{i-1}v_{i-1} - q_iv_i, \\ \frac{dv_N}{dt} = g_N(S)f_N(P)v_N + q_{N-1}v_{N-1}, \\ \frac{dP}{dt} = -h_0(P)u - \sum_{i=1}^N h_i(P)v_i, \end{cases}$$

$$(2.2) \quad \begin{cases} \frac{dS}{dt} = -\frac{1}{\gamma}g_0(S)f_0(P)u - \frac{1}{\gamma}\sum_{i=1}^N g_i(S)f_i(P)v_i, \\ \frac{du}{dt} = g_0(S)f_0(P)u - q_0u + \tilde{q}_0v_1, \\ \frac{dv_i}{dt} = g_i(S)f_i(P)v_i + q_{i-1}v_{i-1} - \tilde{q}_{i-1}v_i - q_iv_i + \tilde{q}_iv_{i+1}, \\ \frac{dv_N}{dt} = g_N(S)f_N(P)v_N + q_{N-1}v_{N-1} - \tilde{q}_{N-1}v_N, \\ \frac{dP}{dt} = -h_0(P)u - \sum_{i=1}^N h_i(P)v_i, \end{cases}$$

where $i = 1, 2, \dots, N-1$, and $v_0 = u$, u , and v_i are the volume densities of the wild type and mutant populations, respectively; γ is the yield constant. In (2.1) and (2.2), the growth rates of the wild type and mutants are given by $g_0(S)$ and $g_i(S)$, which satisfy $g_0(0) = 0$, $g'_0(S) > 0$, $g_i(0) = 0$, and $g'_i(S) > 0$. The bacteria are assumed to consume the drug while the drug inhibits the growth of bacteria. We denote $h_0(P)$ and $h_i(P)$ as the consumption rates of inhibitor P for the wild type bacteria u and



FIG. 2. Forward mutations between species. Mutant v_i mutates to mutant v_{i+1} with a forward mutation rate q_i , and there are no backward mutations. We have $v_0 = u$ and $i = 0, 1, 2, \dots, N-1$.

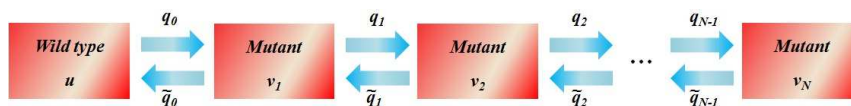


FIG. 3. Forward-backward mutations between species. Mutant v_i mutates to mutant v_{i+1} with a forward mutation rate q_i , while mutant v_{i+1} mutates to mutant v_i with a backward mutation rate \tilde{q}_i . We have $v_0 = u$ and $i = 0, 1, 2, \dots, N-1$.

mutants v_i , respectively. Furthermore, $h_0(P)$ and $h_i(P)$ are nonnegative functions which are increasing in P . The effect of the drug inhibition is described by $f_0(P)$ and $f_i(P)$ and here we use the convention that when $P = 0$, $f_0(0) = 1$ and $f_i(0) = 1$. Meanwhile, $f'_i(P) < 0$ since a larger drug concentration leads to stronger inhibition of the bacteria. Because the mutants have stronger resistance to the inhibitor than the wild type, we have $f_0(P) \leq f_1(P) \leq \dots \leq f_N(P)$. More generally, it is reasonable to assume that the wild type grows more slowly than the mutants in the inhibitor environment, which is our basic assumption as follows:

$$(2.3) \quad g_0(S)f_0(P) < g_1(S)f_1(P) < \dots < g_N(S)f_N(P) \quad \text{for } S \neq 0, P \neq 0;$$

q_i are the forward mutation rates while \tilde{q}_i are the backward mutation rates. We assume that the mutation rates q_i and \tilde{q}_i are quite small compared with the difference of growth rates $g_i(S)f_i(P) - g_{i-1}(S)f_{i-1}(P)$ for all $i = 1, 2, \dots, N$.

The resetting of the nutrient and cells at $t = T_n = nT$ ($n = 0, 1, 2, \dots$) can be written as

$$(2.4) \quad \begin{cases} S(T_n^+) = dS(T_n^-) + (1 - d)S^{(0)}, \\ u(T_n^+) = du(T_n^-), \\ v_i(T_n^+) = dv_i(T_n^-), \end{cases}$$

where $0 < d < 1$ is the dilution ratio of the existing substrate immediately before the dilution step. A fraction, $1 - d$, of the existing substrate is removed and the fresh input substrate of input concentration $S^{(0)}$ is used to refill. As a result, this dilution step contributes a term $(1 - d)S^{(0)}$. T_n^- and T_n^+ denote the time immediately before and after the dilution step at $t = nT$. In mathematical terms, the definitions for T_n^- and T_n^+ are given by

$$T_n^- = \lim_{\epsilon \rightarrow 0^-} nT + \epsilon, \quad T_n^+ = \lim_{\epsilon \rightarrow 0^+} nT + \epsilon.$$

The resetting of the initial condition for the drug concentration P depends on the result from a feedback algorithm. Without the drug injection, the resetting of the initial condition is given by

$$P(T_n^+) = dP(T_n^-).$$

With the drug injection and input drug concentration $P^{(0)}$ during the dilution step, the resetting of the initial condition is given by

$$P(T_n^+) = dP(T_n^-) + (1 - d)P^{(0)}.$$

To be specific, we use a threshold algorithm as an example. The drug injection is invoked if the following condition is fulfilled:

$$(2.5) \quad \left(u + \sum_{i=1}^N v_i \right) (T_n^-) \geq U,$$

where U is the threshold population density.

3. Statement of main results. We first do some simplifications for models (2.1) and (2.2) to make them more mathematically tractable. By scaling $u \rightarrow \frac{u}{\gamma}$, $v_i \rightarrow \frac{v_i}{\gamma}$, $h_0(P) \rightarrow \gamma h_0(P)$, and $h_i(P) \rightarrow \gamma h_i(P)$ for $i = 1, 2, 3, \dots, N$, we obtain the following scaled models of models (2.1) and (2.2), respectively:

$$(3.1) \quad \begin{cases} \frac{dS}{dt} = -g_0(S)f_0(P)u - \sum_{i=1}^N g_i(S)f_i(P)v_i, \\ \frac{du}{dt} = g_0(S)f_0(P)u - q_0u, \\ \frac{dv_i}{dt} = g_i(S)f_i(P)v_i + q_{i-1}v_{i-1} - q_iv_i, \\ \frac{dv_N}{dt} = g_N(S)f_N(P)v_N + q_{N-1}v_{N-1}, \\ \frac{dP}{dt} = -h_0(P)u - \sum_{i=1}^N h_i(P)v_i, \end{cases}$$

$$(3.2) \quad \begin{cases} \frac{dS}{dt} = -g_0(S)f_0(P)u - \sum_{i=1}^N g_i(S)f_i(P)v_i, \\ \frac{du}{dt} = g_0(S)f_0(P)u - q_0u + \tilde{q}_0v_1, \\ \frac{dv_i}{dt} = g_i(S)f_i(P)v_i + q_{i-1}v_{i-1} - \tilde{q}_{i-1}v_i - q_iv_i + \tilde{q}_iv_{i+1}, \\ \frac{dv_N}{dt} = g_N(S)f_N(P)v_N + q_{N-1}v_{N-1} - \tilde{q}_{N-1}v_N, \\ \frac{dP}{dt} = -h_0(P)u - \sum_{i=1}^N h_i(P)v_i, \end{cases}$$

for $T_{n-1} < t < T_n$, and the resetting conditions at $t = T_n$ are

$$(3.3) \quad \begin{cases} S(T_n^+) = dS(T_n^-) + (1-d)S^{(0)}, \\ u(T_n^+) = du(T_n^-), \\ v_i(T_n^+) = dv_i(T_n^-), \\ P(T_n^+) = \begin{cases} dP(T_n^-) & \text{if } (u + \sum_{i=1}^N v_i)(T_n^-) < U, \\ dP(T_n^-) + (1-d)P^{(0)} & \text{if } (u + \sum_{i=1}^N v_i)(T_n^-) \geq U, \end{cases} \end{cases}$$

where $i = 1, 2, \dots, N-1$, and $n = 1, 2, 3, \dots$.

First we state the results about the global dynamics of the morbidostat model with only forward mutations.

THEOREM 3.1. *For the model (3.1) with resetting conditions (3.3), the wild type bacteria u and mutants v_i , $i = 1, 2, 3, \dots, N-1$, go extinct in the long term, i.e., $u_n \rightarrow 0$, $(v_i)_n \rightarrow 0$ as $n \rightarrow \infty$, $i = 1, 2, 3, \dots, N-1$. Furthermore, the following hold:*

- (i) *If $0 < d < \exp(-g_N(S^{(0)})T)$, then $(v_N)_n \rightarrow 0$ and $P_n \rightarrow 0$ as $n \rightarrow \infty$. In other words, all the mutants go extinct, and inhibitor P goes to 0 in the long term in this case.*
- (ii) *If $\exp(-g_N(S^{(0)})T) < d < 1$, then there exist $0 < d_1 < d_2 < 1$ such that*
 - (a) *if $\exp(-g_N(S^{(0)})T) < d < d_1$, then we have $(v_N)_n \rightarrow \tilde{v}_N > 0$ and $P_n \rightarrow 0$ as $n \rightarrow \infty$; in this case, the most resistant microbe v_N will survive while inhibitor P goes to 0 in the long term;*
 - (b) *if $d_2 < d < 1$, then $(v_N)_n \rightarrow \bar{v}_N$, $P_n \rightarrow \bar{P}$ as $n \rightarrow \infty$; in this case, the most resistant microbe v_N and inhibitor P will persist in the morbidostat, and their densities will be \bar{v}_N and \bar{P} ;*
 - (c) *if $d_1 < d < d_2$, the most resistant microbe v_N and inhibitor P will persist in the morbidostat, and their densities may oscillate as the system is trying to maintain a constant bacteria density through feedback.*

Remark 3.2. By persistence of a species we mean continued existence in the deterministic sense, i.e., $\limsup_{t \rightarrow \infty} N(t) > 0$, where $N(t)$ is the population of species N at time t [11].

Theorem 3.1 indicates that the competitive exclusion principle holds when we consider the case with only forward mutation in the morbidostat.

Remark 3.3. From Theorem 3.1, there are three situations in which the most resistant microbe v_N goes extinction, those are

- when the dilution ratio d is small,
- when the the period T is small, or
- when the input nutrient concentration $S^{(0)}$ is small.

Remark 3.4. When the most resistant microbe v_N survives, there are three possible outcomes for inhibitor P :

- There is no inhibitor pumped into the morbidostat, which corresponds to subcase (a) in Theorem 3.1.
- The inhibitor will be pumped into the morbidostat in every dilution cycle, which corresponds to subcase (b) in Theorem 3.1.
- The inhibitor P and most resistant microbe v_N may oscillate, which corresponds to subcase (c) in Theorem 3.1.

Next we consider the case with both of forward and backward mutations.

THEOREM 3.5. *Consider the model (3.2) with resetting conditions (3.3), we have the following:*

- (i) *The wild type bacteria u and mutants $v_i, i = 1, 2, 3, \dots, N$, either go extinct or persist. Furthermore, in the latter case the most resistant microbe v_N dominates the rest of the other species provided the mutation rates \tilde{q}_i are sufficiently small.*
- (ii) *There exist $0 < \hat{d}_1 < \hat{d}_2 < 1$, where $\hat{d}_1 = d_1, \hat{d}_2 > d_2$, such that*
 - (a) *if $0 < d < \hat{d}_1$, then $P_n \rightarrow 0$ as $n \rightarrow \infty$, which indicates there is no inhibitor pumped into morbidostat in the long term;*
 - (b) *if $\hat{d}_2 < d < 1$, then $P_n \rightarrow \bar{P} > 0$ as $n \rightarrow \infty$; in this case, the inhibitor will be pumped into the morbidostat after each dilution cycle in the long term;*
 - (c) *if $\hat{d}_1 < d < \hat{d}_2$, wild type bacteria u , mutant $v_i, i = 1, 2, 3, \dots, N$, and inhibitor P will persist in the morbidostat, and their densities may oscillate as the system is trying to maintain constant bacteria density v_N through feedback. In this case, although the wild type u and the mutants $v_i, i = 1, 2, 3, \dots, N$, persist, the most resistant microbe v_N is in fact dominate provided the mutation rates \tilde{q}_i are sufficiently small.*

Theorem 3.5 indicates that either all species go extinct or all species persist when there are both forward and backward mutations. Remark 3.3 of Theorem 3.1 still holds for Theorem 3.5. On the other hand, due to small backward mutation rates when the species persist, the most resistant species dominates the rest of species. Then Remark 3.4 of Theorem 3.1 still holds for Theorem 3.5. It is noted that $d_2 < \hat{d}_2$, hence the region of hard inhibitor pumping is smaller than the case of forward mutation. This explains why in the operational diagrams the region D in Figure 15 is smaller than that of Figure 14.

Remark 3.6. Theorems 3.1 and 3.5 indicate that the morbidostat selects the most resistant microbe.

4. Numerical simulation. In this section, we summarize the conditions where simulations are done with realistic parameters.

For simplicity, we assume that both the wild type and the mutants have equal uptake function and the growth takes the logistic form, namely,

$$(4.1) \quad g_0(S) = g_i(S) = mS, \quad i = 1, 2, 3, \dots, N.$$

The consumption functions $h_0(P)$ and $h_i(P)$ are assumed to take the Holling Type II function form [11],

$$h_0(P) = h_i(P) = \frac{rP}{a + P}, \quad i = 1, 2, 3, \dots, N.$$

We assume the functions $f_0(P)$ and $f_i(P)$ take the Hill function form of order L , which are

$$(4.2) \quad \begin{cases} f_0(P) = \frac{1}{1 + \left(\frac{P}{K_0}\right)^L}, \\ f_i(P) = \frac{1}{1 + \left(\frac{P}{K_i}\right)^L}, \end{cases}$$

where $i = 1, 2, 3, \dots, N$. Note that the order L stems from the allosteric cooperativity of the drug inhibition [17]. The drug inhibition effects depend on the detailed mechanism. For example, they can result from the binding of the antibiotic drug to the metabolic enzyme that synthesizes the key precursor of biomass production of the bacteria. Taking trimethoprim (TMP) as a specific example, this antibiotic binds to dihydrofolate reductase (DHFR), an enzyme that controls the biosynthesis of folic acid. The mutation of the gene encoding DHFR will modify the binding affinity of TMP [10]. The parameters K_0 and K_i in (4.2) can actually be extracted from the experimental values of IC_{50} , defined as the drug inhibitor concentration at which the growth rate is 50% of the maximal growth rate. The sample volume in the culture vessel of the morbidostat is 10 ml, and the confluent density of *E. Coli* is typically 10^9 cell/ml. For simplicity, we assume that the morbidostat operates at around 10% of the confluent density, which is set by the threshold population U in (2.5). We can conveniently set the yield constant γ to be 1, so that one unit of substrate density will transform to one unit of bacteria. With the volume units set to 0.1 nl, the input substrate $S^{(0)} = 100$ corresponds to 10^9 cell/ml. The constants K_0 and K_i in the drug inhibition function are set to 1 and 10^i , and the order in the Hill function $L = 1, 2, 3$. We first consider the forward mutation rates $q = 10^{-4} \text{hr}^{-1}$. Typically, the dilution ratio $d = 0.9$ and growth period $T = 0.2$ hr are set such that the effective dilution rate $\ln(1-d)/T = 0.5 \text{hr}^{-1}$. The growth rate is set by the constant m to be $8 \times 10^{-3} \text{hr}^{-1}$ in the logistic growth function. The initial conditions are $S(0) = 100, u(0) = 0.01, v(0) = 0$, and $P(0) = 0$. We demonstrate our theoretical results by conducting the following simulations.

4.1. Single mutant with forward mutations. We first assume that there is wild type u and single mutant v in the morbidostat and there is no backward mutation. Then we have the morbidostat model in the following form:

$$(4.3) \quad \begin{cases} \frac{dS}{dt} = -g_0(S)f_0(P)u - g_1(S)f_1(P)v, \\ \frac{du}{dt} = g_0(S)f_0(P)u - qu, \\ \frac{dv}{dt} = g_1(S)f_1(P)v + qv, \\ \frac{dP}{dt} = -h_0(P)u - h_1(P)v \end{cases}$$

for $T_{n-1} < t < T_n$. The resetting conditions at $t = T_n$ ($n = 0, 1, 2, \dots$) can be written as

$$(4.4) \quad \begin{cases} S(T_n^+) = dS(T_n^-) + (1-d)S^{(0)}, \\ u(T_n^+) = du(T_n^-), \\ v(T_n^+) = dv(T_n^-), \\ P(T_n^+) = \begin{cases} dP(T_n^-) & \text{if } (u+v)(T_n^-) < U, \\ dP(T_n^-) + (1-d)P^{(0)} & \text{if } (u+v)(T_n^-) \geq U. \end{cases} \end{cases}$$

Straightforward calculation shows that $\bar{z} = 9.1644$ and $\bar{w} = 28.9818$ by the parameters given above and $P^{(0)} = 3, r = 0.008$, and $a = 0.05$ when $U = 10$.

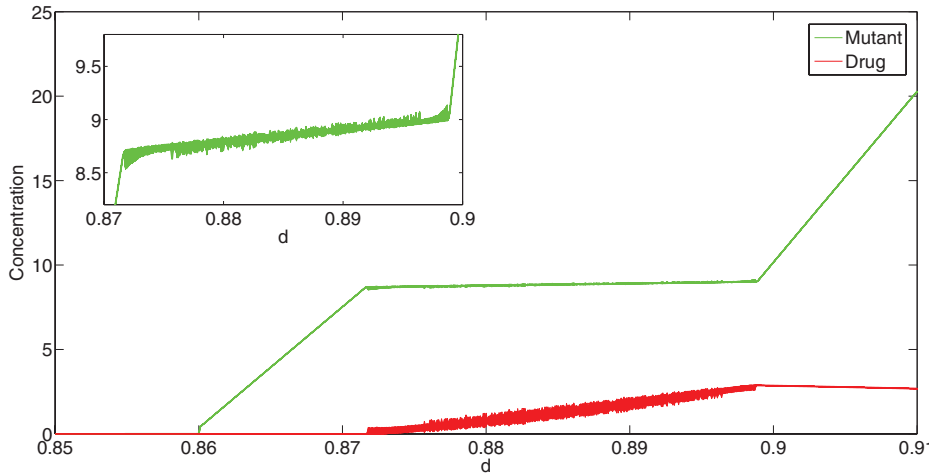


FIG. 4. Equilibrium densities showing the influence of d . In this figure, we fix $U = 10$ and obtain the equilibrium densities of system (4.3) with resetting conditions (4.4) for 5,000 periodic cycles for different dilution ratio d . The mutant densities and the inhibitor concentrations right after the dilution step in the last 200 cycles are plotted. When $d < 0.86$, both the mutant and inhibitor go extinct in the long term; when $0.86 < d < 0.872$, the inhibitor goes extinct while the mutant persists at a fixed level for each d ; when $0.872 < d < 0.899$, both the mutant and inhibitor persists and oscillate for each d ; when $d > 0.899$, both the mutant and inhibitor persist at fixed levels for each d . The inset figure shows the details of mutant densities when d varies from 0.87 to 0.9.

We first fix the threshold $U = 10$ and let the dilution ratio d vary from 0.85 to 0.91; a bifurcation diagram showing the influence of d on the steady states of system (4.3) with resetting conditions (4.4) is demonstrated in Figure 4. In this figure, we simulate the equilibrium densities of system (4.3) with resetting conditions (4.4) for 5,000 periodic cycles for a different dilution ratio d . For each d , the mutant densities and drug concentrations right after the dilution step for the last 200 times are plotted. From Figure 4, we observe that when $d < 0.86$, we have $v_n \rightarrow 0$ and $P_n \rightarrow 0$ as $n \rightarrow \infty$, which means both the mutant and inhibitor go extinct in the long term. For $d \in (0.86, 0.872)$, we have $v_n \rightarrow \tilde{v}(d)$ and $P_n \rightarrow 0$ and as $n \rightarrow \infty$, where $\tilde{v}(d)$ is a constant related to the parameter d . It implies that the mutant will be maintained at a constant concentration which is related to the parameter d , while the inhibitor will vanish in the long term. When d is close to 0.872, the fixed point $(\tilde{v}(d), 0)$ becomes unstable and chaotic for $d \in (0.872, 0.899)$. There is a fixed point (\bar{v}, \bar{P}) for the system (4.3) with resetting conditions (4.4) for $d > 0.899$.

Similarly, if we fix $d = 0.9$, a bifurcation diagram showing the influence of U on the steady states of system (4.3) with resetting conditions (4.4) is demonstrated in Figure 5 for U varies from 0 to 40. We observe that there are three cases for U :

- (i) When $U > \frac{\bar{w}}{\bar{d}} = 32.202$, which satisfies subcase (a) in Theorem 3.1, we have $v_n \rightarrow \bar{w}$ and $P_n \rightarrow 0$ as $n \rightarrow \infty$. More precisely, the fixed point $(\bar{v}, 0) = (\bar{w}, 0) = (28.9819, 0)$ attracts all positive initial data, which agrees well with the theoretical analysis.
- (ii) When $U < \frac{\bar{z}}{\bar{d}} = 10.183$, which satisfies subcase (b) in Theorem 3.1, we have $v_n \rightarrow \bar{v} = 10.1630$ and $P_n \rightarrow \bar{P} = 2.8563$ as $n \rightarrow \infty$. More precisely, there exists a fixed point $(\bar{v}, \bar{P}) = (10.1630, 2.8563)$ for system (4.3) with resetting conditions (4.4) in this case.

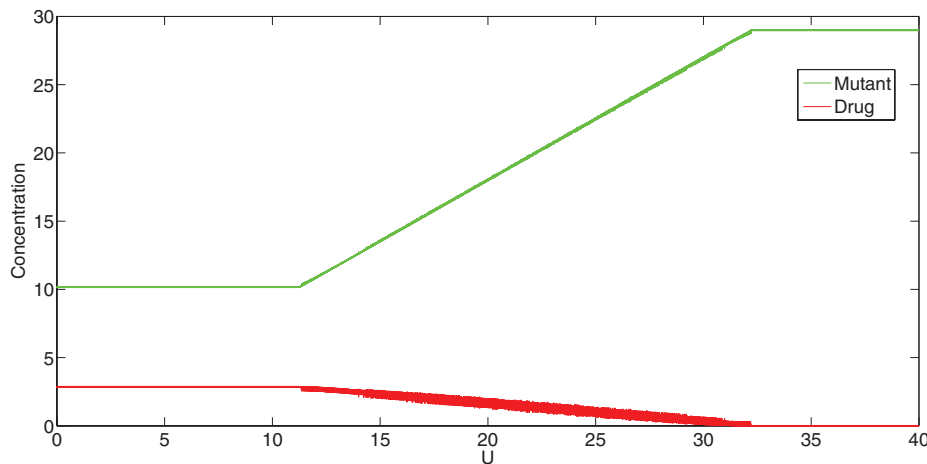


FIG. 5. Equilibrium densities showing the influence of U . In this figure, we fix $d = 0.9$ and obtain the equilibrium densities of system (4.3) with resetting conditions (4.4) for 5,000 periodic cycles for different threshold U . The mutant densities and the inhibitor concentrations right after the dilution step in the last 200 cycles are plotted. When $U < 10.183$, both the mutant and inhibitor persist at fixed levels for each U ; when $10.183 < U < 32.202$, both the mutant and inhibitor persist and oscillate for each U ; when $U > 32.202$, the inhibitor goes extinct while the mutant persists at a fixed level for each U .

- (iii) If $10.183 < U < 32.202$, in this case, we have $\frac{\bar{z}}{d} < U < \frac{\bar{w}}{d}$, which is subcase (c) in Theorem 3.1. From the simulation results, we can see the inhibitor concentration P oscillates between 0 and \bar{P} , which is $P \in (0, 2.8563)$, while the bacteria density v will be maintained nearly constant, and furthermore $v \in (\bar{v}, \tilde{v}) = (10.1630, 28.9819)$.

Next, we demonstrate the long-time dynamics of the morbidostat model using different U in three cases, respectively. We choose $P^{(0)} = 10$ and $d = 0.9$ in the following simulations.

When $U = 33$, it implies $\bar{z} < \bar{w} < dU$, which is subcase (a) in Theorem 3.1. The long-term dynamics of model (4.3) with resetting conditions (4.4) are shown in Figure 6. The insets show the oscillations of the mutant and substrate concentrations in the last 100 dilution steps. As the figure shows, $v_n \rightarrow \bar{w}$ and $P_n \rightarrow 0$ as $n \rightarrow \infty$ in this case. In other words, the fixed point $(\tilde{v}, 0) = (\bar{w}, 0)$ attracts all positive initial data, which verifies Theorem 3.1.

The dynamics of model (4.3) with resetting conditions (4.4) with $U = 10$ is shown in Figure 7. In this case we have $dU < \bar{z} < \bar{w}$, and the two conditions in subcase (b) in Theorem 3.1 can be verified using the parameters given above. The figure shows that $v_n \rightarrow \bar{v}$ and $P_n \rightarrow \bar{P}$ as $n \rightarrow \infty$ in this case. More precisely, there exists a positive fixed point (\bar{v}, \bar{P}) for the morbidostat model (4.3) with resetting conditions (4.4), which agrees well with the result in subcase (b) in Theorem 3.1.

Figure 8 demonstrates the long-term densities of the cells, substrate, and inhibitor of model (4.3) with resetting conditions (4.4) when $U = 15$. In this case, we have $\bar{z} < dU < \bar{w}$, which is subcase (c) in Theorem 3.1. From the simulation results, we can see the inhibitor concentration P oscillates between 0 and \bar{P} , while the bacteria density v will be maintained nearly constant.

To make the situations in subcase (c) in Theorem 3.1 more clear, we choose $P^{(0)} = 10$, $U = 15$, and simulate the morbidostat model (4.3) with resetting conditions (4.4) with some more parameters.

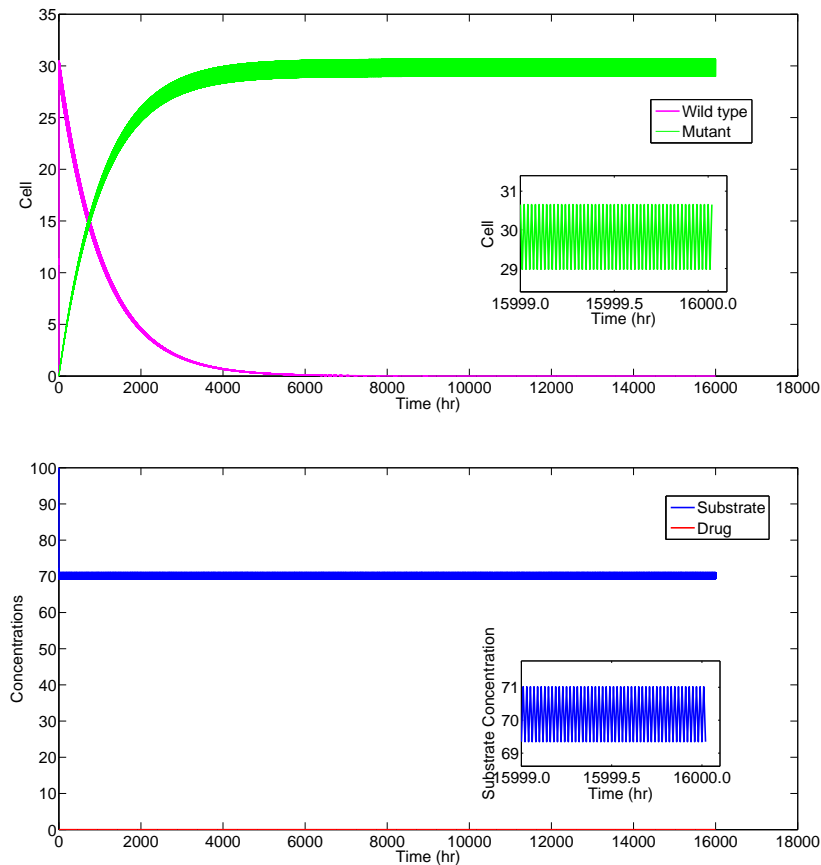


FIG. 6. Cell, substrate, and inhibitor densities of system (4.3) with resetting conditions (4.4) when $U = 33$. The wild type u and inhibitor P go extinct in the morbidostat, while mutant v and substrate S persist at fixed values after each dilution cycle in the long term. The inset figure shows the mutant density (green) and substrate concentration (blue) in the last 100 dilution cycles. In this figure, we use $S^{(0)} = 100$, $T = 0.2$ hr, $d = 0.9$, $q = 10^{-4}$ hr $^{-1}$, $m = 0.008$, $r = 0.008$, $a = 0.05$, $L = 1$, and $K = 10$.

We first fix the mutation rate at $q = 10^{-6}$ hr $^{-1}$ and let L vary from 1 to 3. Both the long-term concentrations of nutrient and inhibitor and the cell densities are shown in Figure 9. It indicates that the mutant v drives u to extinction in each case, and the mutant density is maintained nearly constant. The inhibitor concentration P oscillated between 0 and $P^{(0)}$. As L grows bigger, more inhibitor P is needed to inhibit the bacteria and to maintain v at a nearly constant level. However, the time needed for v to take over is almost the same although the hill functional order L differs.

Next, we fix the hill functional order at $L = 3$ and make the mutation rate q vary from 10^{-4} hr $^{-1}$ to 10^{-8} hr $^{-1}$. Both the concentrations of nutrient and inhibitor and the cell densities are shown in Figure 10. The mutant v still drives u to extinction in each case, and the mutant density is maintained nearly constant. It takes longer for mutant v to take over when the mutation rate is lower. The inhibitor concentration P oscillated between 0 and $P^{(0)}$. And the inhibitor concentration P is almost same although mutation rates are different.

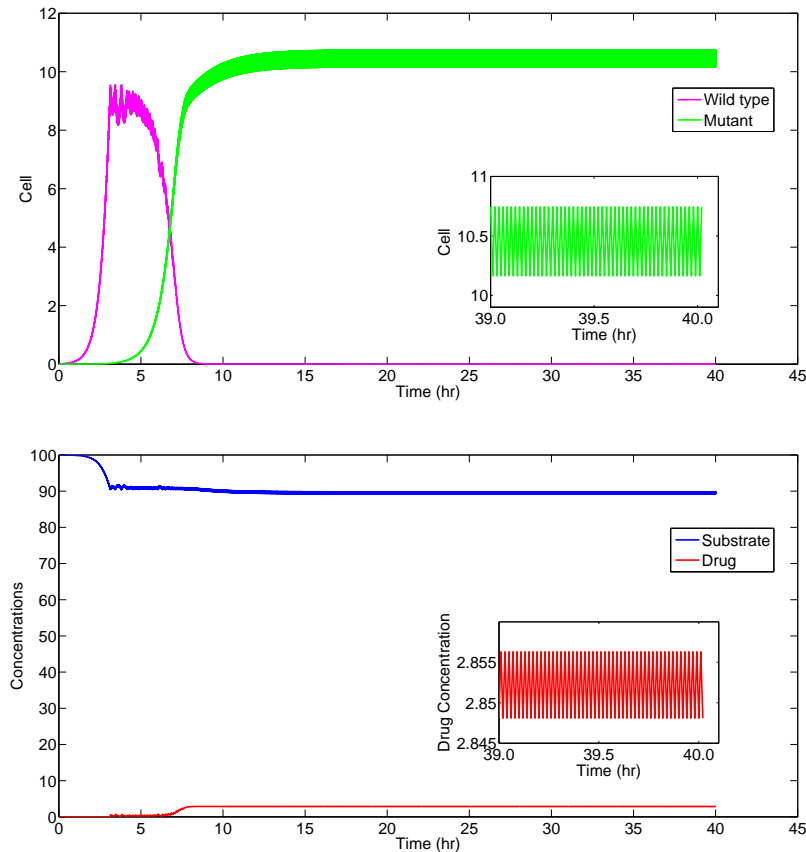


FIG. 7. Cell, substrate, and inhibitor densities of system (4.3) with resetting conditions (4.4) when $U = 10$. The wild type u goes extinct in the morbidostat, while mutant v , substrate S , and inhibitor P persist at fixed values after each dilution cycle in the long term. The inset figure shows the mutant density (green) and inhibitor concentration (red) in the last 100 dilution cycles. In this figure, we use $S^{(0)} = 100$, $T = 0.2$ hr, $d = 0.9$, $q = 10^{-4}$ hr $^{-1}$, $m = 0.008$, $r = 0.008$, $a = 0.05$, $L = 1$, and $K = 10$.

From Figures 6 to 10, we have that the mutant v will drive wild type bacteria u to extinction in the long term no matter what the threshold U is, and no matter how small the mutation rate q and the Hill functional order L is. It shows that the exclusion principle holds, which agrees well with our theoretical analysis in Theorem 3.1.

4.2. Two mutants with both forward and backward mutations. We then assume there is wild type u and two mutants v_1 and v_2 in the morbidostat and assume that the mutants are with forward-backward mutations. Then we have the morbidostat model in the following form:

$$(4.5) \quad \begin{cases} \frac{dS}{dt} = -g_0(S)f_0(P)u - g_1(S)f_1(P)v_1 - g_2(S)f_2(P)v_2, \\ \frac{du}{dt} = g_0(S)f_0(P)u - q_0u + \tilde{q}_0v_1, \\ \frac{dv_1}{dt} = g_1(S)f_1(P)v_1 + q_0u - \tilde{q}_0v_1 - q_1v_1 + \tilde{q}_1v_2, \\ \frac{dv_2}{dt} = g_2(S)f_2(P)v_2 + q_1v_1 - \tilde{q}_1v_2, \\ \frac{dP}{dt} = -h_0(P)u - h_1(P)v_1 - h_2(P)v_2 \end{cases}$$

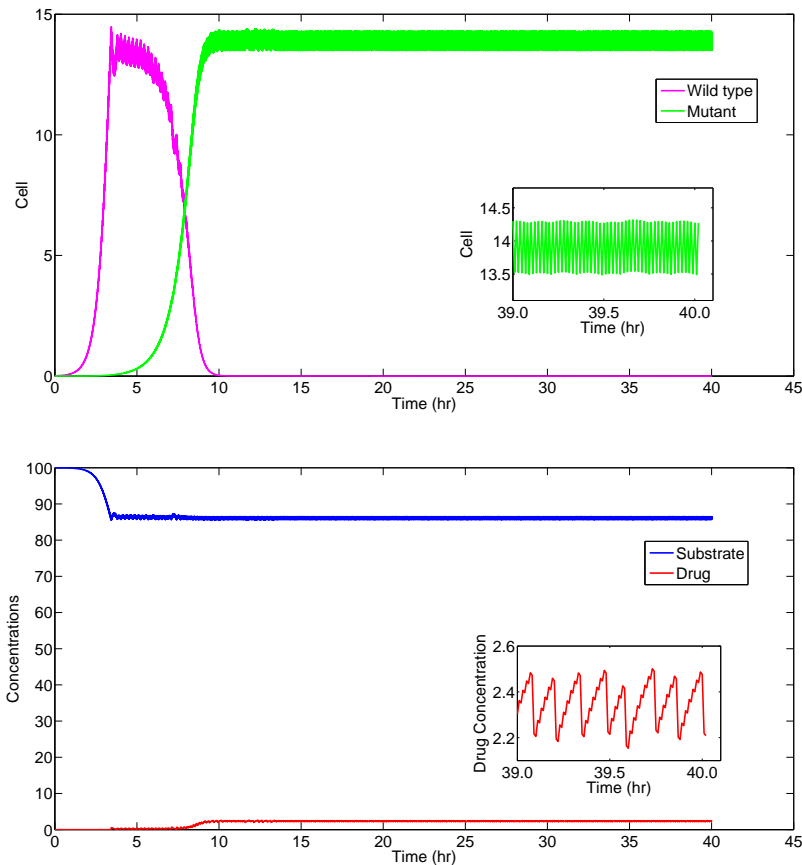


FIG. 8. Cell, substrate, and inhibitor densities of system (4.3) with resetting conditions (4.4) when $U = 15$. The wild type u goes extinct in the morbidostat, while mutant v , substrate S , and inhibitor P oscillate in the long term. The inset figure shows the mutant density (green) and inhibitor concentration (red) in the last 100 dilution cycles. In this figure, we use $S^{(0)} = 100$, $T = 0.2$ hr, $d = 0.9$, $q = 10^{-4}$ hr $^{-1}$, $m = 0.008$, $r = 0.008$, $a = 0.05$, $L = 1$, and $K = 10$.

for $T_{n-1} < t < T_n$. The resetting conditions at $t = T_n$ ($n = 0, 1, 2, \dots$) can be written as

$$(4.6) \quad \begin{cases} S(T_n^+) = dS(T_n^-) + (1-d)S^{(0)}, \\ u(T_n^+) = du(T_n^-), \\ v_1(T_n^+) = dv_1(T_n^-), \\ v_2(T_n^+) = dv_2(T_n^-), \\ P(T_n^+) = \begin{cases} dP(T_n^-) & \text{if } (u + v_1 + v_2)(T_n^-) < U, \\ dP(T_n^-) + (1-d)P^{(0)} & \text{if } (u + v_1 + v_2)(T_n^-) \geq U. \end{cases} \end{cases}$$

The simulation results of system (4.5) with resetting conditions (4.6) show that either all the cells go to extinction (see Figure 11) or persist (see Figures 12 and 13) in the morbidostat, which verifies our theoretical results in Theorem 3.5. In Figure 12, the most resistant mutant dominates the final population with the coexistence of a small fraction of other species (wild type and mutant 1) due to the assumption of small

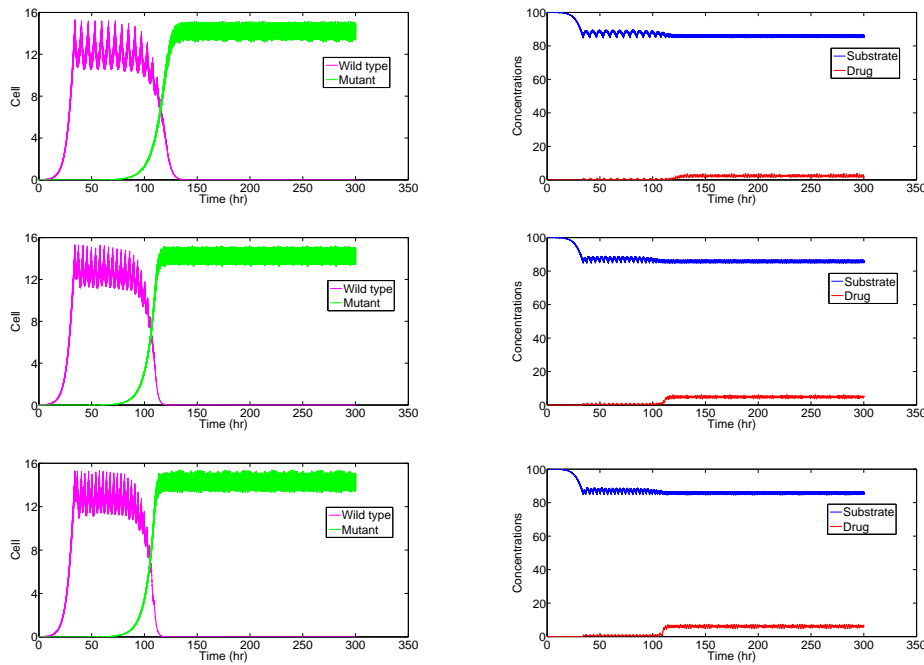


FIG. 9. Cell, substrate, and inhibitor densities of system (4.3) with resetting conditions (4.4) when $L = 1$ (upper panel), 2 (middle panel), and 3 (lower panel), respectively. Wild type u goes extinct in each case, while mutant v persists at a nearly constant level. More inhibitors are needed to maintain the microbes concentration at a nearly constant level as L becomes larger. In this figure, we use $S^{(0)} = 100$, $T = 0.2$ hr, $d = 0.9$, $q = 10^{-6}$ hr $^{-1}$, $m = 0.008$, $r = 0.008$, $a = 0.05$, and $K = 10$.

mutation rates as compared to the growth rates $g_i(S^{(0)})$ ($i = 0, 1, 2$). In Figure 13, the coexistence of all the species is obvious when $q_0 = q_1 = \tilde{q}_0 = \tilde{q}_1 = 0.05$.

4.3. Operation diagrams. Figure 14 presents the operation diagrams of $d-T$, $d-S^{(0)}$, $d-U$, and $d-P^{(0)}$ for experimental use when there are only forward mutations in the morbidostat. In the operation diagrams, logistic growth (4.1) and Hill function (4.2) are used, and $m = 0.008$, $K_0 = 1$, $K_1 = 10$. We assume that there are only forward mutations with a mutation rate $q = 10^{-6}$ hr $^{-1}$. There are four regions in each diagram. Region A is the extinction region where the last mutant v_N goes to extinction. If the parameters fall in region B, then the last mutant v_N survives, while inhibitor P goes to zero in the long term. Region C is the region where the last mutant v_N survives, and inhibitor P oscillates. Region D is the region where the last mutant v_N survives, and inhibitor P goes to a fixed value.

Figure 15 presents the operation diagrams of $d-T$, $d-S^{(0)}$, $d-U$, and $d-P^{(0)}$ for experimental use when there are both forward and backward mutations. The parameters used are the same as in Figure 14, and a backward mutation rate $\tilde{q} = 10^{-6}$ hr $^{-1}$ is considered in these four operation diagrams. In this figure, regions A, B, C, and D have the same interpretations as in Figure 14. It shows that backward mutations do not have any effect on regions A and B. However, they expand region C while shrinking region D in each operation diagram.

5. Conclusion and discussion. In conclusion, we have outlined a mechanistic theory to describe the outcome of microbial growth in a morbidostat. The theory

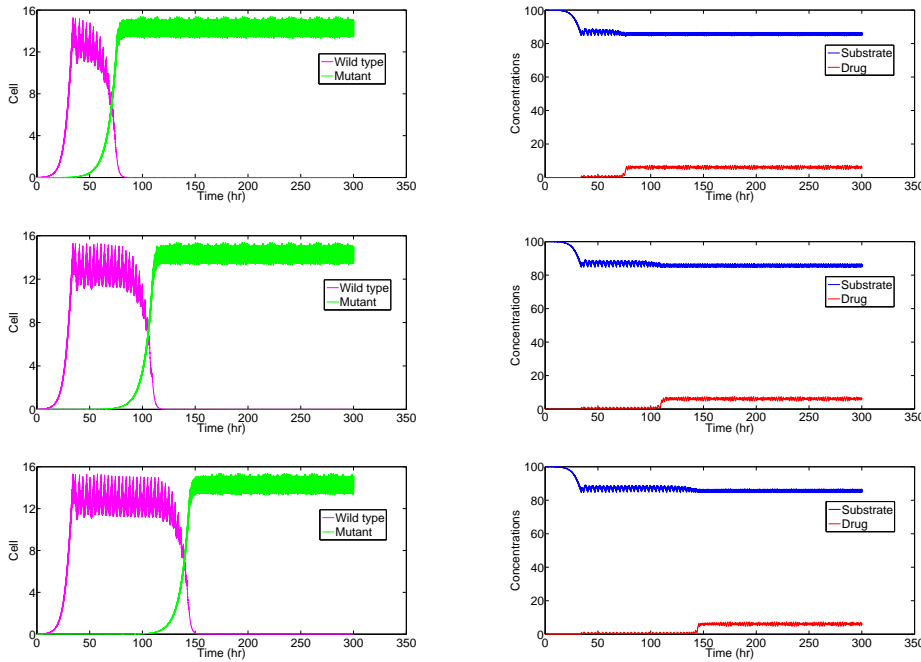


FIG. 10. Cell, substrate, and inhibitor densities of system (4.3) with resetting conditions (4.4) when $q = 10^{-4} \text{ hr}^{-1}$ (upper panel), 10^{-6} hr^{-1} (middle panel), and 10^{-8} hr^{-1} (lower panel), respectively. Wild type u goes extinct in each case, while mutant v persists at a nearly constant level. It takes a longer time for the mutant to take over as the mutation rate becomes lower. In this figure, we use $S^{(0)} = 100$, $T = 0.2 \text{ hr}$, $d = 0.9$, $m = 0.008$, $r = 0.008$, $a = 0.05$, $L = 3$, and $K = 10$.

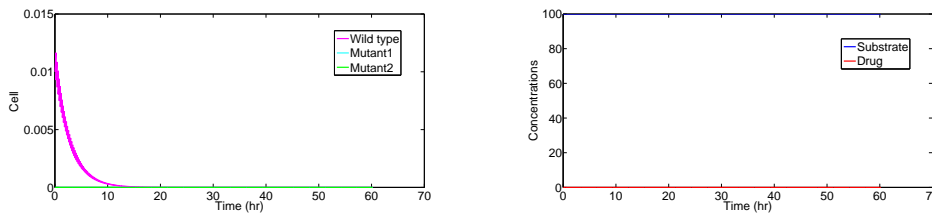


FIG. 11. Extinction of all the microbes of system (4.5) with resetting conditions (4.6). In this case, all the cells and inhibitor go to extinction in the morbidostat, while the substrate persists at a fixed level. In this figure, we use $S^{(0)} = 100$, $T = 0.2 \text{ hr}$, $d = 0.8$, $q_0 = q_1 = \tilde{q}_0 = \tilde{q}_1 = 10^{-4} \text{ hr}^{-1}$, $m = 0.008$, $r = 0.008$, $a = 0.05$, $L = 1$, $K_0 = 3$, and $K_1 = 10$.

incorporates a simple threshold algorithm to recapitulate the feedback effects due to antibiotic drug inhibition. In the simplest scenario, we considered the case of sequential evolution with only forward mutation. This model serves as a concrete example for different modes of operation of the morbidostat. The global dynamics were discussed for three cases. The main result of Theorem 3.1 for case (i) describes a total washout if $0 < d < \exp(-g_N(S^{(0)})T)$, as expected from a serial dilution transfer cultivation [12]. And there are three possible outcomes when the most resistant mutant survives, which are stated in case (ii). Subcase (a) describes the dilution of the drug and survival of the most resistant mutant. Subcase (b) describes a system that is

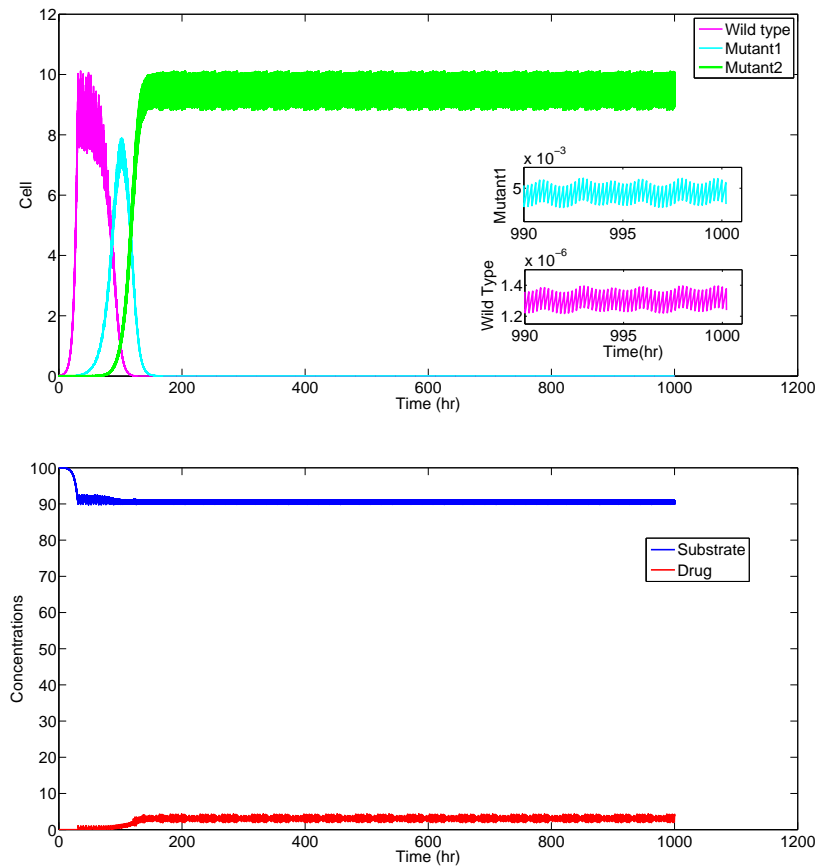


FIG. 12. Persistence of all the microbes of system (4.5) with resetting conditions (4.6). In this case, all the microbes persist in the morbidostat. However, the most resistant microbe dominates all the species. In this figure, we use $S^{(0)} = 100$, $T = 0.2$ hr, $d = 0.9$, $q_0 = q_1 = \tilde{q}_0 = \tilde{q}_1 = 10^{-4}$ hr $^{-1}$, $m = 0.008$, $r = 0.008$, $a = 0.05$, $L = 1$, $K_0 = 3$, and $K_1 = 10$.

trying to pump as hard as possible to suppress the total population. As a result, the final inhibitor concentration asymptotically approached the input inhibitor concentration $P^{(0)}$. Subcase (c) describes the case of oscillation due to the simple threshold feedback used in our analysis. All three subcases were verified using numerical simulations. When backward mutation was included in the evolution of the mutants, the long-term outcome in the morbidostat illustrated the uniform persistence case. We included a simple three-species case to demonstrate these two scenarios.

Although our model considered sequential evolution with mutation, it can be generalized to consider the microbial ecology of a serial transfer dilution bio-reactor with feedback and constant exchange rates between the species. In real experiments, the scenario is much more complicated than the models considered here. In general, it is possible that multiple mutants would be accessible to the wild type species, and a more complicated evolution could be incorporated into the simulations [18]. Experiments could also be conducted to evolve the bacteria so as to acquire not only single drug resistance but also multiple drug resistance. The theory outlined here can

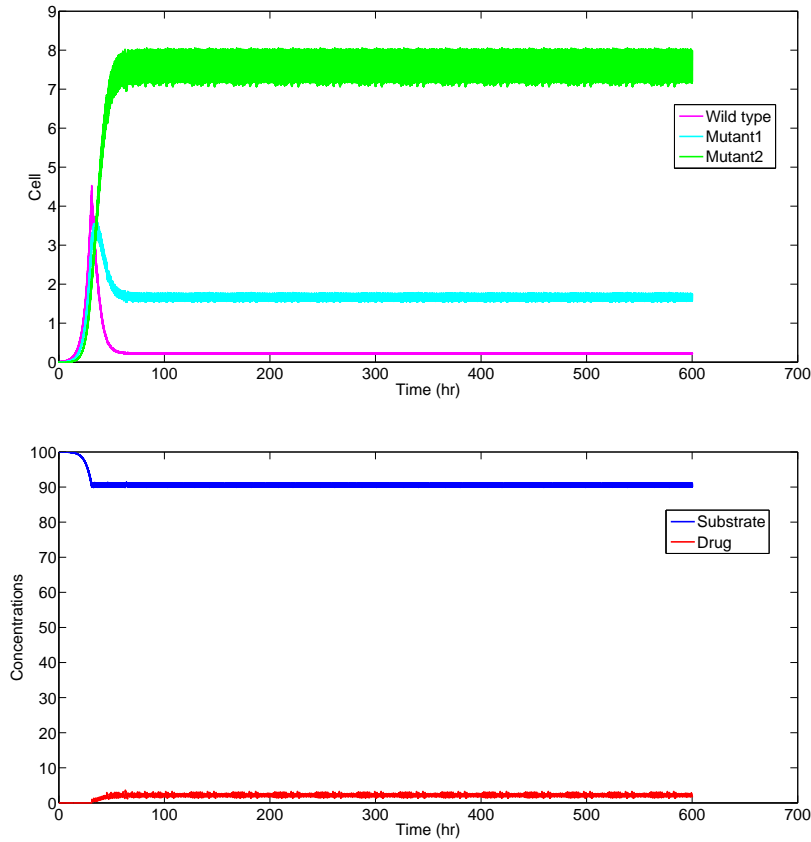


FIG. 13. Persistence of all the microbes of system (4.5) with resetting conditions (4.6). In this case, all the microbes persist in the morbidostat. In this figure, we use $S^{(0)} = 100$, $T = 0.2$ hr, $d = 0.9$, $q_0 = q_1 = \tilde{q}_0 = \tilde{q}_1 = 0.05$ hr⁻¹, $m = 0.008$, $r = 0.008$, $a = 0.05$, $L = 1$, $K_0 = 3$, and $K_1 = 10$.

be generalized to include these scenarios in a straightforward way in the computer simulations. With the theory presented here, one could in principle calculate the population dynamics step by step for a new experiment, or reconcile the experimental results after an experiment has been completed. Finally, our model is deterministic in nature, whereas microbial mutation is stochastic. It will be interesting to generalize our model or simulation to take account of the stochastic nature of the mutation [8].

Appendix A. For the scaled models (3.1) and (3.2) with resetting conditions (3.3), we have the following results.

LEMMA A.1. *The total population density of the nutrient and bacteria in the morbidostat converges to $S^{(0)}$. In other words, we have $S(T_n^+) + u(T_n^+) + \sum_{i=1}^N v_i(T_n^+) \rightarrow S^{(0)}$ as $n \rightarrow \infty$.*

LEMMA A.2. *For the system (3.1) and (3.2) with resetting conditions (3.3), there exists some $\delta > 0$ such that $S(t) \geq \delta > 0$ for all $t \geq 0$.*

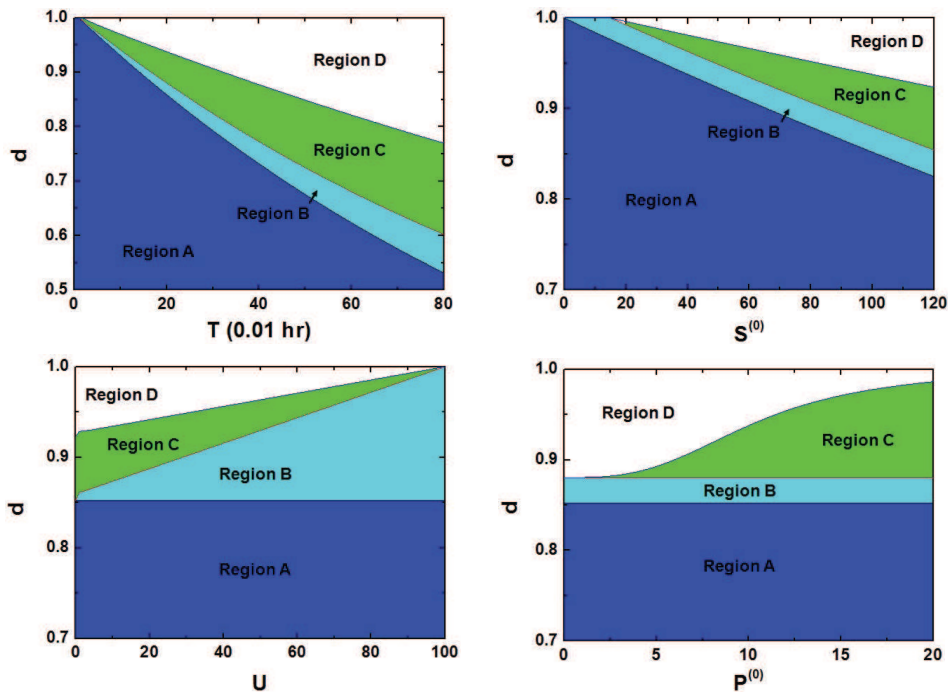


FIG. 14. Operation diagrams when there are only forward mutations: Region A is the extinction region where all the species go to extinction; Region B is the region where only the most resistant microbe survives; Region C is the region where the most resistant microbe survives and inhibitor oscillates; Region D is the region where the most resistant microbe survives and inhibitor persists at a fixed value.

Lemma A.1 states a conservation of species, while Lemma A.2 is a technical lemma.

Proof of Lemma A.1.

Proof. Add the first $N + 2$ equations of models (3.1) and (3.2) together, respectively, and define

$$C(t) = S(t) + u(t) + \sum_{i=1}^N v_i(t);$$

then the following single equation is obtained:

$$C'(t) = S'(t) + u'(t) + \sum_{i=1}^N v_i'(t) = 0 \quad \text{for } 0 < t < T.$$

It follows at once that

$$C(t) = C(0) = C(T_1^-) \quad \text{for } 0 < t < T.$$

Together with the resetting condition at $t = T$, this leads to

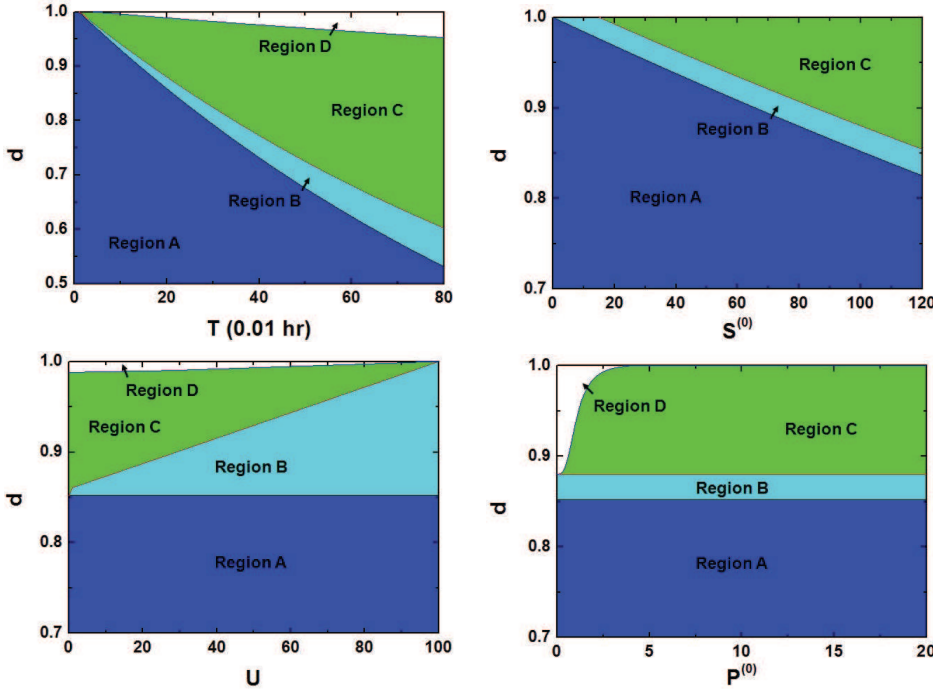


FIG. 15. Operation diagrams when there are both forward and backward mutations: Region A is the extinction region where all the species go to extinction; Region B is the region only the most resistant microbe survives; Region C is the region that the most resistant microbe survives and inhibitor oscillates; Region D is the region that the most resistant microbe survives and inhibitor persists at a fixed value.

$$\begin{aligned}
 C(T_1^+) &= S(T_1^+) + u(T_1^+) + \sum_{i=1}^N v_i(T_1^+) \\
 &= dS(T_1^-) + (1-d)S^{(0)} + du(T_1^-) + \sum_{i=1}^N dv_i(T_1^-) \\
 &= dC(T_1^-) + (1-d)S^{(0)} = dC(0) + (1-d)S^{(0)}.
 \end{aligned}$$

Similarly, the total population density of nutrient S and bacteria u and v_i right after the second period takes the following form:

$$\begin{aligned}
 C(T_2^+) &= dC(T_1^+) + (1-d)S^{(0)} \\
 &= d^2C(0) + (1-d)(1+d)S^{(0)}.
 \end{aligned}$$

Let $C_n = C(T_n^+)$ be the total population following the n th dilution cycle. Then,

$$C_n = C(T_n^+) = d^n C(0) + (1-d)(1+d+\dots+d^{n-1})S^{(0)}.$$

It implies $C_n = S_n + u_n + \sum_{i=1}^N (v_i)_n \rightarrow S^{(0)}$ as $n \rightarrow \infty$, and

$$(A.1) \quad S(t) + u(t) + \sum_{i=1}^N v_i(t) \equiv C_n \rightarrow S^{(0)}$$

for all $t \in [T_n, T_{n+1}]$ as $n \rightarrow \infty$. That completes our proof. \square

Proof of Lemma A.2.

Proof. For the morbidostat models (3.1) and (3.2) with condition (3.3), we have

$$\begin{aligned} \frac{dS}{dt} &= -g_0(S)f_0(P)u - \sum_{i=1}^N g_i(S)f_i(P)v_i \\ &\geq -g_N(S)f_N(P) \left(u + \sum_{i=1}^N v_i \right) \\ &\geq -g_N(S) \left(u + \sum_{i=1}^N v_i \right) \end{aligned}$$

for $t \in [T_n^+, T_{n+1}]$. From (A.1), for any $\varepsilon > 0$ and $t \in [T_n^+, T_{n+1}]$, there exists large enough $J_0 = J_0(\varepsilon) > 0$ such that $n \geq J_0$ implies that

$$(A.2) \quad S^{(0)} - S(t) - \varepsilon < u(t) + \sum_{i=1}^N v_i(t) < S^{(0)} - S(t) + \varepsilon.$$

Therefore, for $t \in [T_n^+, T_{n+1}^+]$, we have

$$(A.3) \quad \begin{cases} \frac{dS}{dt} > -g_N(S)(S^{(0)} - S(t) + \varepsilon), \\ S(T_n^+) > (1-d)S^{(0)}. \end{cases}$$

Let $S^*(t)$ be the solution of the following system:

$$(A.4) \quad \begin{cases} \frac{dS}{dt} = -g_N(S)(S^{(0)} - S(t) + \varepsilon), \\ S(0) = (1-d)S^{(0)}. \end{cases}$$

Then we have $S(t) > S^*(t)$ for all $t \in [T_n^+, T_{n+1}^+]$, $n \geq J_0$. Choose $\delta > 0$ such that $\delta < \min_{0 \leq t \leq T} \{S^*(t)\}$ and $\delta < \min_{0 \leq t \leq T_{J_0}} \{S(t)\}$; we then have $S(t) > \delta$ for all $t \geq 0$. That completes our proof. \square

Define a map Q by

$$(A.5) \quad Q(S_0, u_0, (v)_0, P_0) = (S_1, u_1, (v)_1, P_1),$$

where $v = (v_1, v_2, \dots, v_N)$, $S_1 = dS(T, S_0, u_0, (v)_0, P_0) + (1-d)S^{(0)}$, $u_1 = du(T, S_0, u_0, (v)_0, P_0)$, $(v)_1 = dv(T, S_0, u_0, (v)_0, P_0)$, $P_1 = P(T^+, S_0, u_0, (v)_0, P_0)$, and $(S(t, S_0, u_0, (v)_0, P_0), u(t, S_0, u_0, (v)_0, P_0), v(t, S_0, u_0, (v)_0, P_0), P(t, S_0, u_0, (v)_0, P_0))$ are the solutions of (3.1) or (3.2) with initial conditions $S(0) = S_0, u(0) = u_0, (v)(0) = (v)_0, P(0) = P_0$.

Let $S_n = S(T_n^+), u_n = u(T_n^+), (v)_n = (v)(T_n^+), P_n = P(T_n^+)$ be the values of the vector of the population densities immediately following the n th dilution cycle; then

$$(A.6) \quad Q(S_n, u_n, (v)_n, P_n) = (S_{n+1}, u_{n+1}, (v)_{n+1}, P_{n+1}), \quad n = 1, 2, 3, \dots$$

Global dynamics of the morbidostat model without backward mutations. Consider the case of the forward mutations (3.1) with the resetting conditions (3.3); we have the following competitive exclusion results.

LEMMA A.3. *The wild type bacteria u and mutants v_i , where $1 \leq i \leq N-1$, go extinct in the long term. More precisely, $u_n \rightarrow 0, (v_i)_n \rightarrow 0$ as $n \rightarrow \infty, 1 \leq i \leq N-1$.*

Proof of Lemma A.3.

Proof. From model (3.1), if letting $\omega(t) = u(t) + v_1(t) + v_2(t) + \dots + v_{N-1}(t)$, it is easy to check that

$$\frac{d\omega}{dt} = g_0(S)f_0(P)u + g_1(S)f_1(P)v_1 + \dots + g_{N-1}(S)f_{N-1}(P)v_{N-1} - q_{N-1}v_{N-1}.$$

Since $g_0(S)f_0(P) \leq g_1(S)f_1(P) \leq \dots \leq g_{N-1}(S)f_{N-1}(P)$ for all $0 < S \leq S^{(0)}$ and $0 \leq P \leq P^{(0)}$, we have

$$(A.7) \quad \frac{d\omega}{\omega} \leq \left(g_{N-1}(S)f_{N-1}(P) - q_{N-1} \frac{v_{N-1}}{\omega} \right) dt.$$

Integrating both sides of (A.7) over the interval $(0, T)$,

$$\int_{\omega(0)}^{\omega(T)} \frac{d\omega}{\omega} \leq \int_0^T \left(g_{N-1}(S)f_{N-1}(P) - q_{N-1} \frac{v_{N-1}}{\omega} \right) dt.$$

This implies

$$(A.8) \quad \frac{\omega_1}{\omega_0} \leq d \exp \left(\int_0^T g_{N-1}(S)f_{N-1}(P) dt \right) \exp \left(-q_{N-1} \int_0^T \frac{v_{N-1}}{\omega} dt \right),$$

where $u(0) + v_1(0) + \dots + v_{N-1}(0) = \omega_0$, $du(T) + dv_1(T) + \dots + dv_{N-1}(T) = \omega_1$ as defined. Similarly, for the last mutants v_N , we have the following equation:

$$(A.9) \quad \frac{(v_N)_1}{(v_N)_0} = d \exp \left(\int_0^T g_N(S)f_N(P) dt \right) \exp \left(q_{N-1} \int_0^T \frac{v_{N-1}}{v_N} dt \right).$$

Multiply (A.8) by (A.9); it is easy to check

$$\begin{aligned} \frac{\omega_1}{\omega_0} &= \frac{(v_N)_1}{(v_N)_0} \exp \left(\int_0^T (g_{N-1}(S)f_{N-1}(P) - g_N(S)f_N(P)) dt \right) \exp \left(-q_{N-1} \int_0^T \frac{v_{N-1}}{\omega} dt \right) \\ &\quad \exp \left(-q_{N-1} \int_0^T \frac{v_{N-1}}{v_N} dt \right) \\ &\leq \frac{(v_N)_1}{(v_N)_0} \exp \left(\int_0^T (g_{N-1}(S)f_{N-1}(P) - g_N(S)f_N(P)) dt \right). \end{aligned}$$

We apply the same technique during the second periodic cycle $(T, 2T)$; then the following inequality is obtained:

$$\frac{\omega_2}{\omega_1} \leq \frac{(v_N)_2}{(v_N)_1} \exp \left(\int_T^{2T} (g_{N-1}(S)f_{N-1}(P) - g_N(S)f_N(P)) dt \right).$$

Similarly, during the i th periodic cycle $((i-1)T, iT)$, we have

$$\frac{\omega_i}{\omega_{i-1}} \leq \frac{(v_N)_i}{(v_N)_{i-1}} \exp \left(\int_{(i-1)T}^{iT} (g_{N-1}(S)f_{N-1}(P) - g_N(S)f_N(P)) dt \right),$$

where $i = 1, 2, 3, \dots, n$. Multiply both sides of all the inequalities above; we have

$$\frac{\omega_n}{\omega_0} \leq \frac{(v_N)_n}{(v_N)_0} \exp \left(\int_0^{nT} (g_{N-1}(S)f_{N-1}(P) - g_N(S)f_N(P))dt \right).$$

Since $S(t) \geq \delta > 0$ for all $t > 0$ and $g_{N-1}(S(t))f_{N-1}(P(t)) < g_N(S(t))f_N(P(t))$, we have $\omega_n \rightarrow 0$ as $n \rightarrow \infty$ since $(v_N)_n \leq S^{(0)}$. Therefore $u_n \rightarrow 0$ and $(v_i)_n \rightarrow 0$ as $n \rightarrow \infty$ for $1 \leq i \leq N - 1$. \square

From Lemmas A.1 and A.3, the forward mutation morbidostat model (3.1) with resetting conditions (3.3) can be reduced to the following limiting system:

$$(A.10) \quad \begin{cases} \frac{dv_N}{dt} = g_N(S^{(0)} - v_N)f_N(P)v_N & \text{for } T_{n-1} < t < T_n, \\ \frac{dP}{dt} = -h_N(P)v_N & \text{for } T_{n-1} < t < T_n, \end{cases}$$

with resetting conditions at $t = T_n$,

$$(A.11) \quad \begin{cases} v_N(T_n^+) = dv_N(T_n^-), \\ P(T_n^+) = \begin{cases} dP(T_n^-) & \text{if } v_N(T_n^-) < U, \\ dP(T_n^-) + (1 - d)P^{(0)} & \text{if } v_N(T_n^-) \geq U. \end{cases} \end{cases}$$

We denote $(v_N(t), P(t))$ as the solution of model (A.10) with resetting conditions (A.11), and $((v_N)_n, P_n) = (v_N(T_n^+), P(T_n^+))$. The long-term dynamics of the morbidostat model is our concern. In order to analyze the dynamics of the morbidostat, we will first study two comparison systems.

Since

$$f_N(P^{(0)}) < f_N(P) \leq 1$$

for $0 \leq P < P^{(0)}$, the first comparison system to be studied is as follows:

$$(A.12) \quad \begin{cases} \frac{dw}{dt} = g_N(S^{(0)} - w)w & \text{for } T_{n-1} < t < T_n, \\ w(T_n^+) = dw(T_n^-) & \text{for } t = T_n. \end{cases}$$

Let $w(t)$ be the solution of the problem (A.12) and denote w_n as the population density right after the n th dilution cycle; then we know $w_n = w(T_n^+)$. Let $x_0 = w_0$, and define map Q_1 by $Q_1(x_0) = Q_1(w_0) = w_1 = dw(T, w_0)$. Denote $\Phi_t(x_0) = (w(t, w_0))$ as the solution of the following equation:

$$(A.13) \quad \frac{dw}{dt} = g_N(S^{(0)} - w)w$$

with initial condition $w(0) = w_0$.

We will next study the existence and stability of the fixed point of system (A.12). Based on the results in [14], we have the following results.

LEMMA A.4. For system (A.12),

- (i) if $0 < d < \exp(-g_N(S^{(0)}T))$, then the extinction fixed point $\bar{w} = 0$ is globally attracting;
- (ii) if $\exp(-g_N(S^{(0)}T) < d < 1$, then there is a unique positive fixed point $\bar{w} > 0$ satisfying $Q_1(\bar{w}) = \bar{w}$ and it attracts all positive initial data; in other words, $Q_1(w_n) \rightarrow \bar{w} > 0$, for all $w(0) \in (0, S^{(0)})$.

The second comparison system is as follows:

$$(A.14) \quad \begin{cases} \frac{dz}{dt} = g_N(S^{(0)} - z)f_N(P^{(0)})z & \text{for } T_{n-1} < t < T_n, \\ z(T_n^+) = dz(T_n^-) & \text{for } t = T_n. \end{cases}$$

We denote $z(t)$ as the solution of problem (A.14) and $z_n = z(T_n^+)$ as the population density right after the n th dilution cycle. Define map Q_2 by $Q_2(z_0) = z_1 = dz(T, z_0)$. For system (A.14), we have a similar result as the first comparison system. The post-dilution density sequence z_n converges to a fixed point, $z_n \rightarrow \bar{z}$, where $Q_2(\bar{z}) = \bar{z}$. This fixed point may or may not be the trivial fixed point $\bar{z} = 0$. And the stability of the fixed point can be given by the following lemma.

LEMMA A.5. *For system (A.14), we have the following two results:*

- (i) *If $0 < d < \exp(-g_N(S^{(0)})f_N(P^{(0)})T)$, then the extinction fixed point $\bar{z} = 0$ is globally attracting.*
- (ii) *If $\exp(-g_N(S^{(0)})f_N(P^{(0)})T) < d < 1$, then there is a unique positive fixed point $\bar{z} > 0$ satisfying $Q_2(\bar{z}) = \bar{z}$ and it attracts all positive initial data, in other words, $Q_2(z_n) \rightarrow \bar{z} > 0$ for all $z(0) \in (0, S^{(0)})$. Furthermore, at the fixed point we have $d \exp(\int_0^T g_N(S^{(0)} - z(t, \bar{z}))f_N(P^{(0)})dt) = 1$.*

Since

$$g_N(S^{(0)} - v) f(P^{(0)})v < g_N(S^{(0)} - v) f(P)v \leq g_N(S^{(0)} - v)v,$$

from (A.10), (A.12), and (A.14), it follows that

$$z_n < (v_N)_n \leq w_n.$$

Therefore, we have $\bar{z} \leq (v_N)_n \leq \bar{w}$ for n sufficiently large.

For the fixed points of system (A.12) and (A.14) $\bar{w} = \bar{w}(d)$, $\bar{z} = \bar{z}(d)$, we have the following results.

LEMMA A.6. *Let $U < S^{(0)}$:*

- (i) *$\bar{w}(d)$ and $\bar{z}(d)$ satisfy $\bar{w}(1) = \bar{z}(1) = S^{(0)}$, $\bar{w}(d_w^*) = \bar{z}(d_z^*) = 0$, where $d_w^* = \exp\{-g_N(S^{(0)})T\}$, $d_z^* = \exp\{-g_N(S^{(0)})f_N(P^{(0)})T\}$, and hence $d_w^* < d_z^*$.*
- (ii) *Both $\frac{\bar{w}(d)}{d}$ and $\frac{\bar{z}(d)}{d}$ are strictly increasing in d .*
- (iii) *There exist $0 < d_1 < d_2 < 1$ such that $\frac{\bar{w}(d_1)}{d_1} = U$ and $\frac{\bar{z}(d_2)}{d_2} = U$.*

Proof of Lemma A.4.

Proof. Clearly, $Q_1(0) = 0$ and Q_1 is strictly increasing by uniqueness of solutions of the initial value problem (A.13). Because $w = S^{(0)}$ is an equilibrium of (A.13), we have

$$Q_1(S^{(0)}) = dS^{(0)} < S^{(0)},$$

which implies

$$0 < \dots < w_{n+1} < w_n < w_{n-1} < \dots < S^{(0)}$$

for all $n \geq 1$. Therefore, the postdilution density sequence converges to a fixed point, $w_n \rightarrow \bar{w}$, where $Q_1(\bar{w}) = \bar{w}$. This fixed point may or may not be the trivial fixed point $\bar{w} = 0$. The stability of the fixed point is determined by

$$Q_1'(x_0) = D_{x_0}Q_1(x_0).$$

Then the stability of the trivial fixed point is determined by

$$Q_1'(0) = d \frac{\partial w}{\partial w_0}(T, 0),$$

where $x(t) = \frac{\partial w}{\partial w_0}(t)$ satisfies the variational equation

$$x' = xg_N(S^{(0)}), \quad x(0) = 1.$$

Noticing that $Q_1'(0) = d \exp(\int_0^T g_N(S^{(0)}) dt) > 0$. The trivial fixed point is asymptotically stable if $Q_1'(0) < 1$ and unstable if $Q_1'(0) > 1$. That completes our proof. \square

Proof of Lemma A.6.

Proof. (i) As $d = 1$, from (A.12) and (A.14) it follows that $w_n \rightarrow S^{(0)}$, $z_n \rightarrow S^{(0)}$ as $n \rightarrow \infty$. Hence $\bar{w}(1) = \bar{z}(1) = S^{(0)}$. By Lemma A.4(i) and Lemma A.5(i), we have $\bar{w}(d_w^*) = 0$ and $\bar{z}(d_z^*) = 0$, where d_w^* and d_z^* are defined as above.

(ii) In order to prove $\frac{\bar{w}(d)}{d}$ is a strictly increasing function of d , we will first prove $\bar{w}(d)$ is a strictly increasing function of d . Since \bar{w} is the fixed point of model (A.12), we have

$$(A.15) \quad \bar{w}(d) = dw(T, \bar{w}).$$

Differentiating both sides of (A.15) with respect to d , yields

$$(A.16) \quad \bar{w}'(d) = \frac{w(T, \bar{w})}{1 - d \frac{\partial w(T, \bar{w})}{\partial \bar{w}}}.$$

From (A.16), if $1 - d \frac{\partial w(T, \bar{w})}{\partial \bar{w}} > 0$, then $\bar{w}'(d) > 0$. Since

$$(A.17) \quad \frac{dw(t, w_0)}{dt} = g_N(S^{(0)} - w(t, w_0)) w(t, w_0)$$

for $t \in (0, T)$, differentiating both sides of (A.17) with respect to w_0 , we have

$$\left\{ \begin{array}{l} \frac{d}{dt} \frac{\partial w(t, w_0)}{\partial w_0} = \frac{\partial w(t, w_0)}{\partial w_0} [g_N(S^{(0)} - w(t, w_0)) - g'_N(S^{(0)} - w(t, w_0)) w(t, w_0)], \\ \frac{\partial w}{\partial w_0}(0, w_0) = 1. \end{array} \right.$$

Therefore,

$$(A.18) \quad \frac{\partial w(t, w_0)}{\partial w_0} > 0$$

and

$$\begin{aligned} \frac{\partial w(T, w_0)}{\partial w_0} &= \exp\left(\int_0^T (g_N(S^{(0)} - w(t, w_0)) - g'_N(S^{(0)} - w(t, w_0)) w(t, w_0)) dt\right) \\ &< \exp\left(\int_0^T (g_N(S^{(0)} - w(t, w_0))) dt\right) \\ &= \frac{1}{d}. \end{aligned}$$

Then, we have

$$(A.19) \quad \frac{\partial \bar{w}(d)}{\partial d} = \frac{w(T, \bar{w})}{1 - d \frac{\partial w(T, \bar{w})}{\partial \bar{w}}} > 0.$$

It implies $\bar{w}(d)$ is a strictly increasing function of d . Since $\frac{\bar{w}(d)}{d} = w(T, \bar{w})$, by the chain rule, we have

$$\left(\frac{\bar{w}(d)}{d}\right)' = \frac{\partial w(T, \bar{w})}{\partial d} = \frac{\partial w(T, \bar{w})}{\partial \bar{w}} \frac{\partial \bar{w}}{\partial d}.$$

Therefore, from (A.18) and (A.19) we have $(\frac{\bar{w}(d)}{d})' > 0$.

By applying the same procedure to the second comparison system (A.14), we have $\frac{\bar{z}(d)}{d}$ is also an increasing function of d .

The proof of (iii) follows directly from (i) and (ii) and the assumption $U < S^{(0)}$. That completes our proof. \square

We will now study the dynamics of the solution of the limiting system (A.10) with resetting conditions (A.11). According to the relations of fixed points \bar{z}, \bar{w} , and threshold U , we have the main results in the following three cases.

Case 1: No drug inhibitor case of the limiting system. If $d < d_1$, we have $\bar{z} < \bar{w} \leq dU$, and hence $(v_N)_n \leq dU$ for all large n , then the inhibitor P dilutes in every dilution cycle. Therefore, there is no inhibitor pumped into the morbidostat. And the inhibitor concentration P_n takes the form after the n th dilution cycle,

$$P_n < dP_{n-1} < \dots < d^n P_0,$$

since $h_i(P) \geq 0$ for $i = 1, 2, 3, \dots, N$. From $0 < d < 1$, it is obvious that $P_n \rightarrow 0$ as $n \rightarrow \infty$. System (A.10) with resetting condition (A.11) can be reduced to the limiting system (A.12). Thus, in this case, we have $(v_N)_n \rightarrow \bar{w}$ as $n \rightarrow \infty$. More precisely, we have the following results.

LEMMA A.7. *For the limiting system (A.10) with resetting conditions (A.11), when $d < d_1$,*

- (i) *if $0 < d < \exp(-g_N(S^{(0)})T)$, then the extinction fixed point $(0, 0)$ is globally attracting;*
- (ii) *if $\exp(-g_N(S^{(0)})T) < d < d_1$, then there is a unique $\tilde{v}_N > 0$ satisfying $Q(\tilde{v}_N, 0) = (\tilde{v}_N, 0)$ and the fixed point $(\tilde{v}_N, 0)$ attracts all positive initial data; in other words, $Q((\tilde{v}_N)_n, P_n) \rightarrow (\tilde{v}_N, 0)$ for all $v_N(0) \in (0, S^{(0)})$, and $P(0) \in (0, P^{(0)})$.*

Remark A.8. Note that if $0 < d < \exp(-g_N(S^{(0)})T)$, this is simply the trivial case of total washout. If $\exp(-g_N(S^{(0)})T) < d < d_1$, the system will end up with zero drug inhibitor concentration. Nevertheless, the last mutant wins. This result is simply due to the assumption of forward mutation. The system will have drug inhibitor on to drive all the mutant population into the most resistant mutant survival case.

Case 2: Hard inhibitor pumping of the limiting system. If $d > d_2$, we have $dU < \bar{z} \leq \bar{w}$, and hence $(v_N)_n > dU$ for all large n . In this case, the inhibitor P will be pumped into the morbidostat in every dilution cycle. In other words, the resetting of inhibitor P will always follow the rule $P_n = dP(nT) + (1 - d)P^{(0)}$ for $n = 1, 2, 3, \dots$. Thus, after the n th dilution cycle, the inhibitor concentration P_n satisfies

$$\begin{aligned} P_n &< dP_{n-1} + (1 - d)P^{(0)} \\ &< d^2P_{n-2} + (1 - d)(1 + d)P^{(0)} \\ &< \dots \\ &< d^n P_0 + (1 - d)(1 + d + \dots + d^{n-1})P^{(0)} \end{aligned}$$

since $h_i(P) \geq 0$ for $i = 1, 2, 3, \dots, N$. It implies $P_n < P^{(0)}$ as $n \rightarrow \infty$. In this case, system (A.10) with resetting condition (A.11) can be reduced to the following limiting system:

$$(A.20) \quad \begin{cases} \frac{dv_N}{dt} = g_N(S^{(0)} - v_N)f_N(P)v_N & \text{for } T_{n-1} < t < T_n, \\ \frac{dP}{dt} = -h_N(P)v_N & \text{for } T_{n-1} < t < T_n, \\ v_N(T_n^+) = dv_N(T_n^-) & \text{for } t = T_n, \\ P(T_n^+) = dP(T_n^-) + (1-d)P^{(0)} & \text{for } t = T_n, \end{cases}$$

where $n = 1, 2, 3, \dots$. We will first study the existence of positive fixed points of system (A.20), then analyze the stability of the positive fixed point.

It is easy to check that system (A.20) is a competitive system; then by Lemma 2.2 in [15], we have the following result. For any initial value $((v_N)_0, P_0) \in R_+^2$, the sequence of point $Q^n((v_N)_0, P_0)$ converges to a fixed point of Q as $n \rightarrow \infty$. Without loss of generality, we denote this fixed point as (\bar{v}_N, \bar{P}) . Since $(v_N)_n > dU$ for n large, we have $\bar{v}_N > 0$ and $\bar{P} > 0$. Therefore, there exists a positive fixed point (\bar{v}_N, \bar{P}) for system (A.20), and it satisfies the following conditions.

Remark A.9. If $h_N(P) = 0$, i.e., the last mutant does not consume inhibitor, then it is easy to verify that $\bar{P} = P^{(0)}$ and $P_n \rightarrow P^{(0)}$ as $n \rightarrow \infty$. Then we consider the limiting system (A.14) from Lemma A.5, and the dynamical behavior of $\{(v_N)_n\}_{n=1}^\infty$ follows.

Let $(v_N(t, \bar{v}_N), P(t, \bar{P}))$ be the solutions of system (A.20) with initial value (\bar{v}_N, \bar{P}) ; then

$$dv_N(T, \bar{v}_N) = \bar{v}_N$$

and

$$dP(T, \bar{P}) + (1-d)P^{(0)} = \bar{P}.$$

Case 3: Oscillation of the limiting system. If $d_1 < d < d_2$, we have $\bar{z} < dU < \bar{w}$ in this case. Thus the resetting of P will follow the dilution rule $P_n = dP_{n-1}$ if $(v_N)_{n-1} < dU$; otherwise it will follow the resetting rule $P_n = dP_{n-1} + (1-d)P^{(0)}$. Therefore, the inhibitor concentration may oscillate in this case as the system is trying to maintain constant bacteria density v_N through feedback. We also demonstrate it by numerical simulation in section 4.

Proof of Theorem 3.1. Based on the above analysis, we complete the proof of Theorem 3.1. \square

Global dynamics of the morbidostat model with both forward and backward mutations. When there are both forward and backward mutations in the morbidostat, we have the following lemmas and main results in two cases.

LEMMA A.10. *If $(v_j)_n \rightarrow 0$ as $n \rightarrow \infty$ for some j , $0 \leq j \leq N$, then $(v_k)_n \rightarrow 0$ as $n \rightarrow \infty$ for all $k \neq j$, and $0 \leq k \leq N$. This result indicates that wild type and all the mutants will go to extinction if any one of them go to extinction in the long term.*

THEOREM A.11. *For the morbidostat model with both forward and backward mutations (3.2) with resetting conditions (3.3), and A is the $(N+1) \times (N+1)$ matrix in (A.29), we have the following:*

- (i) *If the spectral radius $r(\text{dexp}(AT)) < 1$, then $(S_n, u_n, (v)_n, P_n) \rightarrow E_0$ as $n \rightarrow \infty$, where $E_0 = (S^{(0)}, 0, 0, \dots, 0)$. In this case, the wild type and all the mutants go extinct in the long term.*
- (ii) *If the spectral radius $r(\text{dexp}(AT)) > 1$, then the system (3.2) with resetting conditions (3.3) is persistent. In this case, all the species coexist in the morbidostat in the long term. Furthermore, the last mutant v_N dominates the rest of the other species if the backward mutation rates are sufficiently small.*

When all the species coexist in the morbidostat, we study the density of the cells by studying two comparison systems. Let $\mu(t) = u(t) + v_1(t) + v_2(t) + \dots + v_N(t)$; then for the cells in the morbidostat, we have

$$(A.21) \quad \begin{cases} \frac{d\mu}{dt} = g_0(S)f_0(P)u + \sum_{i=1}^N g_i(S)f_i(P)v_i & \text{for } T_{n-1} < t < T_n, \\ \mu(T_n^+) = d\mu(T_n^-) & \text{for } t = T_n. \end{cases}$$

To study the limiting system (A.21), by hypothesis (2.3) we introduce two comparison systems of it. The first comparison system is (A.12), which is the same one as in Appendix A. The second comparison system takes the form of

$$(A.22) \quad \begin{cases} \frac{d\kappa}{dt} = g_0(S^{(0)} - \kappa)f_0(P^{(0)})\kappa & \text{for } T_{n-1} < t < T_n, \\ \kappa(T_n^+) = d\kappa(T_n^-) & \text{for } t = T_n. \end{cases}$$

We denote $\kappa(t)$ as the solution of problem (A.22) and $\kappa_n = \kappa(T_n^+)$ as the population density right after the n th dilution cycle. Define map Q_3 by $Q_3(\kappa_0) = \kappa_1 = d\kappa(T, \kappa_0)$. For system (A.22), we have a similar result as the comparison systems (A.12) and (A.14). The postdilution density sequence κ_n converges to a fixed point, $\kappa_n \rightarrow \bar{\kappa}$, where $Q_3(\bar{\kappa}) = \bar{\kappa}$. This fixed point may or may not be the trivial fixed point $\bar{\kappa} = 0$. And the stability of the fixed point can be given by the following lemma.

LEMMA A.12. *For system (A.22), we have the following two results:*

- (i) *If $0 < d < \exp(-g_0(S^{(0)})f_0(P^{(0)})T)$, then the extinction fixed point $\bar{\kappa} = 0$ is globally attracting.*
- (ii) *If $\exp(-g_0(S^{(0)})f_0(P^{(0)})T) < d < 1$, then there is a unique positive fixed point $\bar{\kappa} > 0$ satisfying $Q_3(\bar{\kappa}) = \bar{\kappa}$ and it attracts all positive initial data; in other words, $Q_3(\kappa_n) \rightarrow \bar{\kappa} > 0$ for all $\kappa(0) \in (0, S^{(0)})$. Furthermore, at the fixed point we have $d \exp(\int_0^T g_0(S^{(0)} - \kappa(t, \bar{\kappa}))f_0(P^{(0)})dt) = 1$.*

It follows that

$$\kappa_n < \mu_n \leq w_n.$$

Therefore, we have $\bar{\kappa} \leq \mu_n \leq \bar{w}$ for n sufficiently large.

For the fixed points of system (A.12) and (A.22) $\bar{w} = \bar{w}(d)$, $\bar{\kappa} = \bar{\kappa}(d)$, we have the following results.

LEMMA A.13. *Let $U < S^{(0)}$:*

- (i) *$\bar{w}(d)$ and $\bar{\kappa}(d)$ satisfy $\bar{w}(1) = \bar{\kappa}(1) = S^{(0)}$, $\bar{w}(d_w^*) = \bar{\kappa}(d_w^*) = 0$, where $d_w^* = \exp\{-g_N(S^{(0)})T\}$, $d_\kappa^* = \exp\{-g_0(S^{(0)})f_0(P^{(0)})T\}$, and hence $d_w^* < d_\kappa^*$.*
- (ii) *Both $\frac{\bar{w}(d)}{d}$ and $\frac{\bar{\kappa}(d)}{d}$ are strictly increasing in d .*
- (iii) *There exist $0 < \hat{d}_1 < \hat{d}_2 < 1$ such that $\frac{\bar{w}(\hat{d}_1)}{\hat{d}_1} = U$ and $\frac{\bar{\kappa}(\hat{d}_2)}{\hat{d}_2} = U$.*

The proof of Lemma A.13 is similar to the proof of Lemma A.6; therefore we omit the details of the proof here.

Remark A.14. From the basic assumption (2.3), comparing (A.14) with (A.22) yields that $d_2 < \hat{d}_2$. When $d > \hat{d}_2$, we have $dU < \bar{\kappa} < \bar{w}$. Thus $w_n > dU$ for all large n . It implies that the inhibitor P will be pumped into the morbidostat in every dilution cycle in this case.

Proof of Lemma A.10.

Proof. We may assume $0 < j < N$, and the proofs for the cases with $j = 0$ or $j = N$ are the same as that for $0 < j < N$. Since $(v_j)_n \rightarrow 0$ as $n \rightarrow \infty$, then for any $\epsilon > 0$, there exists $N_j > 0$ such that $0 < (v_j)_n < \epsilon$ for $n \geq N_j$. From Lemma A.2

$S(t) \geq \delta > 0$, $0 < P(t) < P^{(0)}$ for all $t > 0$; then $g_j(S(t))f_j(P(t)) - (\tilde{q}_{j+1} + q_j) > 0$ for $t \in [T_n^+, T_{n+1}]$, where q_i and \tilde{q}_i are sufficiently small for $0 \leq i \leq N$.

We have

$$(A.23) \quad \frac{dv_j}{dt} = (g_j(S)f_j(P) - (\tilde{q}_{j-1} + q_j))v_j + (q_{j-1}v_{j-1} + \tilde{q}_jv_{j+1}) > 0,$$

for $t \in [T_n^+, T_{n+1}]$, and $v_j(T_n^+) = (v_j)_n$, $v_j(T_{n+1}) = \frac{1}{d}(v_j)_{n+1}$.

From (A.23) it follows that $v_j(t)$ is strictly increasing on $[T_n^+, T_{n+1}]$ and $0 < v_j(t) < \frac{1}{d}(v_j)_{n+1} < \frac{1}{a}\epsilon$ for $t \in [T_n^+, T_{n+1}]$ and $n \geq N_j$. From (A.23), we have

$$\begin{aligned} \frac{d^2v_j}{dt^2} &= (g_j(S)f_j(P) - (\tilde{q}_{j-1} + q_j))v'_j + (g'_j(S)S'f_j(P) + g_j(S)f'_j(P)P')v_j \\ &\quad + (q_{j-1}v'_{j-1} + \tilde{q}_jv'_{j+1}). \end{aligned}$$

It is easy to verify that from the equations of (3.2) and Lemma A.1, we have

$$|S'| \leq \left(\max_{\delta \leq S \leq S^{(0)}, 0 \leq P < P^{(0)}} \{f_N(P)g_N(S)\} \right) S^{(0)}$$

and

$$|v'_{j-1}|, |v'_j|, |v'_{j+1}| \leq \left(\max_{\delta \leq S \leq S^{(0)}, 0 \leq P < P^{(0)}} \{f_N(P)g_N(S)\} + \max_{0 \leq i \leq N} \{\tilde{q}_{i-1} + q_i\} \right) S^{(0)}.$$

Since $|g_j(S)f_j(P)| \leq (\max_{\delta \leq S \leq S^{(0)}, 0 \leq P < P^{(0)}} \{f_N(P)g_N(S)\})$, and $f'_j(P) < 0$, we have $|\frac{d^2v_j}{dt^2}| \leq M_j$ for some $M_j > 0$. Let $|\frac{dv_j}{dt}|$ take its maximum in $[T_n^+, T_{n+1}]$ at $t = \xi$. If $T_n < \xi < T_{n+1}$, then we choose a, b such that $a \leq \xi \leq b$, $(a, b) \subset (T_n, T_{n+1})$, and $b - a = \sqrt{\epsilon}$. By the arguments in [15],

$$(A.24) \quad v_j(b) - v_j(\xi) = (b - \xi)v'_j(\xi) + \frac{1}{2}(b - \xi)^2v''_j(\eta_1),$$

$$(A.25) \quad v_j(a) - v_j(\xi) = (a - \xi)v'_j(\xi) + \frac{1}{2}(a - \xi)^2v''_j(\eta_2),$$

where $a < \eta_2 < \xi < \eta_1 < b$.

Subtracting (A.25) from (A.24), we get

$$v_j(b) - v_j(a) - (b - a)v'_j(\xi) = \frac{1}{2}[v''_j(\eta_1)(b - \xi)^2 - v''_j(\eta_2)(a - \xi)^2].$$

Since $(b - \xi)^2 + (a - \xi)^2 \leq (b - a)^2$, $a \leq \xi \leq b$, it follows that $|v'_j(\xi)| \leq \frac{|v_j(b)| + |v_j(a)|}{b - a} + \frac{1}{2}M_j(b - a) \leq \frac{\frac{2}{\sqrt{\epsilon}} + \frac{M_j}{2}\sqrt{\epsilon}}{\sqrt{\epsilon}} = \sqrt{\epsilon}(\frac{2}{\sqrt{\epsilon}} + \frac{M_j}{2})$.

Hence on $[T_n^+, T_{n+1}]$, from (A.23), $\sqrt{\epsilon}(\frac{2}{\sqrt{\epsilon}} + \frac{M_j}{2}) \geq (g_j(S)f_j(P) - (\tilde{q}_{j-1} + q_j))v_j + q_{j-1}v_{j-1} + \tilde{q}_jv_{j+1} \geq O(1)\epsilon + q_{j-1}v_{j-1} + \tilde{q}_jv_{j+1}$. Therefore, when $t = T_{n+1}$, we have $q_{j-1}\frac{1}{d}(v_{j-1})_{n+1} + \tilde{q}_j\frac{1}{d}(v_{j+1})_{n+1} \leq O(1)\sqrt{\epsilon}$ for $n \geq N_j$. Hence, we have $(v_{j-1})_n, (v_{j+1})_n \rightarrow 0$ as $n \rightarrow \infty$.

If $\xi = nT$ or $(n + 1)T$, then we consider (A.25) with $\xi = a$, $b - a = \sqrt{\epsilon}$ or $\xi = b$, $b - a = \sqrt{\epsilon}$, respectively. Following the same procedure we are able to prove $(v_{j-1})_n, (v_{j+1})_n \rightarrow 0$ as $n \rightarrow \infty$. That completes our proof. \square

Proof of Theorem A.11.

Proof. (i) Compare the model (3.2) with resetting conditions (3.3) with the following system (A.26) with resetting conditions (3.3):

$$(A.26) \quad \begin{cases} \frac{dS}{dt} = 0, \\ \frac{du}{dt} = g_0(S)u - q_0u + \tilde{q}_0v_1, \\ \frac{dv_i}{dt} = g_i(S)v_i + q_{i-1}v_{i-1} - \tilde{q}_{i-1}v_i - q_iv_i + \tilde{q}_iv_{i+1}, \\ \frac{dv_N}{dt} = g_N(S)v_N + q_{N-1}v_{N-1} - \tilde{q}_{N-1}v_N, \\ \frac{dP}{dt} = 0. \end{cases}$$

By letting $X = (S, u, v_1, \dots, v_N, P)$, we write (3.2) as $\frac{dX}{dt} = F(X)$ and (A.26) as $\frac{dX}{dt} = G(X)$. It is obvious that $F(X) \leq G(X)$. Note that (A.26) is a cooperative system; by Kamke’s theorem, we have

$$(A.27) \quad (S_n, u_n, (v)_n, P_n) \leq (\hat{S}_n, \hat{u}_n, (\hat{v})_n, \hat{P}_n),$$

where $(\hat{S}_n, \hat{u}_n, (\hat{v})_n, \hat{P}_n) = \hat{Q}^{(n)}(\hat{S}_0, \hat{u}_0, (\hat{v})_0, \hat{P}_0)$, and $(\hat{S}_0, \hat{u}_0, (\hat{v})_0, \hat{P}_0) = (S_0, u_0, (v)_0, P_0)$. Consider the extinction fixed point $(S^{(0)}, 0, 0, \dots, 0, 0)$ of the system (A.26) with resetting conditions (3.3); we have $\hat{S}_n \rightarrow S^{(0)}$ as $n \rightarrow \infty$. Then we study the limiting system of the cooperative system (A.26) with resetting conditions (3.3),

$$(A.28) \quad \begin{cases} \frac{du}{dt} = g_0(S^{(0)})u - q_0u + \tilde{q}_0v_1, \\ \frac{dv_i}{dt} = g_i(S^{(0)})v_i + q_{i-1}v_{i-1} - \tilde{q}_{i-1}v_i - q_iv_i + \tilde{q}_iv_{i+1}, \\ \frac{dv_N}{dt} = g_N(S^{(0)})v_N + q_{N-1}v_{N-1} - \tilde{q}_{N-1}v_N. \end{cases}$$

Let $x = (u, v_1, \dots, v_N)$; then (A.28) can be written as

$$\frac{dx}{dt} = Ax,$$

where

$$(A.29) \quad A = \begin{bmatrix} A_{11} & \tilde{q}_0 & 0 & 0 & 0 & \dots & 0 \\ q_0 & A_{22} & \tilde{q}_1 & 0 & 0 & \dots & 0 \\ 0 & q_1 & A_{33} & \tilde{q}_2 & 0 & \dots & 0 \\ \dots & \dots & \dots & \dots & \dots & \dots & \dots \\ 0 & \dots & 0 & 0 & 0 & q_{N-1} & A_{N+1N+1} \end{bmatrix},$$

$A_{ii} = g_{i-1}(S^{(0)}) - (\tilde{q}_{i-2} + q_{i-1})$ for $i = 2, 3, \dots, N$, $A_{11} = g_0(S^{(0)}) - q_0$, and $A_{N+1N+1} = g_N(S^{(0)}) - \tilde{q}_{N-1}$. Since the mutation rates q_i and \tilde{q}_i are small for $0 \leq i \leq N$, $\tilde{q}_{i-1} + q_i < g_i(S^{(0)})$ for all $1 \leq i \leq N$. Then from the map induced by (A.28) and (3.3),

$$\tilde{Q}\vec{x}_0 = d \exp(AT)\vec{x}_0,$$

it follows that

$$\vec{x}_n = \tilde{Q}^n \vec{x}_0 = (d \exp(AT))^n \vec{x}_0.$$

Since A is a positive matrix, if the spectral radius $r(d \exp(AT))$ is less than 1, then $\vec{x}_n \rightarrow 0$ as $n \rightarrow \infty$, or $(\hat{u}_n, (\hat{v})_N) \rightarrow (0, 0, \dots, 0)$ as $n \rightarrow \infty$. In this case, by (A.27) we have $(u_n, (v)_N) \rightarrow (0, 0, \dots, 0)$ as $n \rightarrow \infty$.

(ii) We will prove the persistence of models (3.2) and (3.3) in the following two cases.

Case 1. If $u(T_{n+1}) + \sum_{i=1}^N v_i(T_{n+1}) < U$ for all n , then $P_n \rightarrow 0$ as $n \rightarrow \infty$. Since the matrix $d\exp(AT)$ is a positive irreducible matrix, the spectral radius $r(d\exp(AT)) > 1$ is an eigenvalue with positive eigenvalue \vec{w} . Since $E_0 = (S^{(0)}, 0, 0, \dots, 0) \in R^{N+2}$ is the only fixed point on the boundary ∂R^{N+2} , we can verify $W^s(E_0) \cap \text{Int}(R^{N+2}) = \emptyset$. Hence the system (3.2) and (3.3) is persistent.

Case 2. If $u(T_{n+1}) + \sum_{i=1}^N v_i(T_{n+1}) \geq U$ for some $n > 0$. Then the iterates $(S_n, u_n, (v_i)_n, p_n)$ may iterate about the boundary $u + \sum_{i=1}^N v_i = U$. From Lemma A.10, we know that either $(v_i)_n \rightarrow 0$ as $n \rightarrow \infty$ for all $0 \leq i \leq N$ or $(v_i)_n \not\rightarrow 0$ as $n \rightarrow \infty$ for all $0 \leq i \leq N$. Thus if $r(d\exp(AT)) > 1$, the system (3.2) with resetting conditions (3.3) is persistent.

We will next prove that the last mutant v_N dominates the other populations if the backward mutation rates are sufficiently small. Let $(\tilde{S}_n, \tilde{u}_n, (\tilde{v}_i)_n, \tilde{P}_n)$ be the solution of system (3.1) with resetting conditions (3.3). From Lemma A.3, $\tilde{u}_n + \sum_{i=1}^{N-1} (\tilde{v}_i)_n \rightarrow 0$ as $n \rightarrow \infty$. Hence given $\epsilon > 0$, there exists $n_0 > 0$ such that $0 < \tilde{u}_n + \sum_{i=1}^{N-1} (\tilde{v}_i)_n < \epsilon$ for all $n \geq n_0$. Consider the fixed interval $[n_0T, 2n_0T]$ and the solution $(S_n, u_n, (v_i)_n, P_n)$ of the system (3.2) with resetting conditions (3.3). From continuous dependence properties on parameters [16], it follows that if the backward mutation rates $\tilde{q}_0, \tilde{q}_1, \dots, \tilde{q}_{N-1}$ are sufficiently close to 0, then $|(S_n, u_n, (v_i)_n, P_n) - (\tilde{S}_n, \tilde{u}_n, (\tilde{v}_i)_n, \tilde{P}_n)| < \epsilon$ for all $n \in [n_0, 2n_0]$. It implies that $0 < u_n + \sum_{i=1}^{N-1} (v_i)_n < 2\epsilon$ for $n \in [n_0, 2n_0]$. Since all the species u, v_1, \dots, v_N coexist in the morbidostat, we have that the last mutant v_N dominates the population $u + \sum_{i=1}^{N-1} v_i$. That completes our proof. \square

Proof of Theorem 3.5. By Theorem A.11, Lemma A.12, Lemma A.13, and Remark A.14, we complete the proof of Theorem 3.5. \square

REFERENCES

- [1] S. B. LEVY AND B. MARSHALL, *Antibiotic resistance worldwide: Causes, challenges, and responses*, Nat. Med., 10 (2004), pp. s122–s129.
- [2] M. BARBER, *Infection by penicillin resistant Staphylococci*, Lancet, 2 (1948), pp. 641–644.
- [3] M. MWANGI, S. W. WU, Y. ZHOU, ET AL., *Tracking the in vivo evolution of multidrug resistance in Staphylococcus aureus by whole genome sequencing*, Proc. Natl. Acad. Sci. USA, 104 (2007), pp. 9451–9456.
- [4] M. DRAGOSITS AND D. MATTANOVICH, *Adaptive laboratory evolution—principles and applications for biotechnology*, Micro. Cell Fact., 12 (2013), 64.
- [5] Q. ZHANG, G. LAMBERT, D. LIAO, H. KIM, K. ROBIN, C. TUNG, N. POURMAND, AND R. H. AUSTIN, *Acceleration of emergence of bacterial antibiotic resistance in connected microenvironment*, Science, 333 (2011), pp. 1764–1767.
- [6] R. HERMSEN, J. B. DERIS, AND T. HWA, *On the rapidity of antibiotic resistance evolution facilitated by a concentration gradient*, Proc. Natl. Acad. Sci. USA, 109 (2012), pp. 10775–10780.
- [7] R. HERMSEN AND T. HWA, *Sources and Sinks: A Stochastic Model of Evolution in Heterogeneous Environments*, Phys. Rev. Lett., 105 (2010), 248104.
- [8] J. B. DERIS, M. KIM, Z. ZHANG, H. OKANO, R. HERMSEN, A. GROISMAN, AND T. HWA, *The innate growth bistability and fitness landscapes of antibiotic resistant bacteria*, Science, 342 (2013), 1237435.
- [9] H. L. SMITH AND P. E. WALTMAN, *The Theory of the Chemostat*, Cambridge University Press, Cambridge, UK, 1995.
- [10] E. TOPRAK, A. VERES, J. B. MITCHEL, D. L. HARTL, AND R. KISHONY, *Evolutionary paths to antibiotic resistance under dynamically sustained drug selection*, Nature Genet., 44 (2012), pp. 101–106.
- [11] H. L. SMITH AND H. R. THIEME, *Dynamical Systems and Population Persistence*, AMS, Providence, RI, 2011.

- [12] H. L. SMITH, *Bacterial competition in serial transfer culture*, Math. Biosci., 229 (2011), pp. 149–159.
- [13] S. B. HSU AND P. E. WALTMAN, *Analysis of a model of two competitors in a chemostat with an external inhibitor*, SIAM J. Appl. Math., 52 (1992), pp. 528–540.
- [14] S. B. HSU AND X. Q. ZHAO, *A Lotka-Volterra competition model with seasonal succession*, J. Math. Biol., 64 (2012), pp. 109–130.
- [15] W. A. COPPEL, *Stability and Asymptotic Behavior of Differential Equations*, Health Math. Monogr., Heath, Boston, 1965.
- [16] S. B. HSU, *Ordinary Differential Equations with Applications*, Word Scientific, River Edge, NJ, 2006.
- [17] A. URI, *An Introduction to System Biology Design Principles of Biological Circuits*, Chapman and Hall, London, 2007.
- [18] A. C. PALMER, E. TOPRAK, M. BAYM, S. KIM, A. VERES, S. BERSHTEIN, AND R. KISHONY, *Delayed Commitment to Evolutionary Fate in Antibiotic Resistance Fitness Landscapes*, Nature Commun., 6 (2015), <https://doi.org/10.1038/ncomms8385>.